International Journal of Multidisciplinary Research and Growth Evaluation.

Red Planet, Green Thumb

Massimo Iavernaro
Liceo Scientifico di Stato "G. Battaglini", Corso Umberto I n. 106, Taranto, Italy

* Corresponding Author: **Massimo Iavernaro**

Article Info

ISSN (online): 2582-7138
Volume: 06
Issue: 01
January-February 2025
Received: 06-12-2024
Accepted: 09-01-2025
Page No: 1855-1877

Abstract
Space agencies are actively exploring solutions for sustaining human life on Mars, including the cultivation of plants in extreme environments. This article presents a high school educational experiment designed to engage students in interdisciplinary science by simulating plant growth under martian conditions, using a purpose-built martian regolith simulant (MSP-1). Using martian regolith simulant as a substrate, the study examines the growth patterns of broad beans (*Vicia faba maior*), chosen for their nitrogen-fixing properties, rapid growth, and ease of measurement. Key parameters analyzed include growth rates, leaf area development, and biomass production. The primary objectives of this experiment are twofold: to provide students with hands-on experience in applying scientific methods to real-world challenges and to stimulate their interest in space exploration and sustainability. While the results do not aim to introduce groundbreaking discoveries, they highlight key challenges associated with extraterrestrial agriculture and offer insights into adapting terrestrial practices for martian environments. By replicating this experiment, educators can inspire students to connect classroom knowledge with innovative problem-solving approaches, fostering critical thinking and collaboration skills. This work underscores the value of integrating practical experiments into science education and contributes to ongoing discussions on the feasibility of sustainable agriculture beyond Earth.

DOI: https://doi.org/10.54660/.IJMRGE.2025.6.1-1855-1877

Keywords: Astrobiology, cultivation on mars, Martian regolith simulant

1. Introduction

1.1 Objectives

The objective of this work is to explore the opportunities and challenges associated with the cultivation of plants on Mars, an environment that is not conducive for life as it is known on Earth. In particular, attention is paid to the broad bean (Vicia faba maior), a legume selected for its nitrogen-fixing properties and for the ease of measuring some growth parameters. This study focuses on plant response in a semi-controlled environment, using a martian regolith simulant as substrate.

Growing plants under such conditions presents several challenges. Crop failure could lead to food shortages, highlighting the need for effective strategies, equipment, and techniques adapted to the environmental conditions of Mars to prevent such failures and ensure the safety and quality of the food produced. Another important aspect that emerges is the positive impact that plant cultivation can have on the psychological health of colonists [1, 2].

Several studies have shown that Mars regolith simulants (MRS) are able to support the growth of a wide range of plants: asparagus, garlic, carrot, watercress, alfalfa, lettuce, legumes, ryegrass, bell pepper, tomato, quinoa, turnip, radish, arugula, rye, spinach and various wild plants such as common groundnut. The JSC Mars-1 and MMS simulants have had varying degrees of success with and without any fertilizer additions. The highly alkaline MGS-1 simulant negatively affected the growth of sweetpotato [3], while its acidification almost doubled the longevity of the plants [4-7]. The presence of nitrogen in the atmosphere of Mars (2.7%) has led to experiments with nitrogen-fixing legumes by exploiting the symbiotic plant-microbe (*rhizobium*) association [8, 9].

1.2 Martian simulants produced for astrobiology

An important limitation of any simulant is that there is no "universal" that fully represents the mineralogy of the surface Martian. Just as the surface of Earth is heterogeneous, so is the surface of Mars and it is therefore difficult to replicate all the features of regolith in a single simulant, consequently several groups have developed simulants designed to be more mineralogically and chemically accurate and include phyllosilicates, sulfates, and other important phases, but many are not widely available in sufficient volumes for plant growth studies. In any case, no existing simulants contain enough water or organic components to support plant growth in the absence of nutrient supplementation [10].

However, specific aspects of the design, construction, and materials of the simulant used as components can affect the structure soil, salinity, pH, and potential nutrient extractability, all of which are features essential needed to better understand the feasibility of using Mars soil for plant cultivation.

Listed below are martian soil analogs suitable for experiments of astrobiology.

MGS-1 (Mars Global Simulant) developed at the CLASS Exolith Lab (https://sciences.ucf.edu/class/exolithlab/) [11], intended as a mineralogical standard of the Martian soil, useful in many applications and available for distribution.

UF Acid-Alkaline-Salt Basalt Analog Soils are simulants made in six different versions by the University of Florida and the Johnson Space Center for experiments concerning the survival of microbial colonies in a martian environment simulated. They contain Minnesota basalt, salts, acids, alkalis, aeolians, and perchlorates [12, 13]. These simulants appear to have been used only for this study and were probably created only in small batches without the intent to produce or distribute them.

JMSS-1 (Jining Mars Soil Simulant) was developed at the Lunar and Planetary Science Research Center of the Chinese Academy of Sciences for general purposes. It contains crushed basalt from a crater near the city of Jining in Shandong province. The mineral content consists of plagioclase, pyroxene, olivine, and to a lesser extent ilmenite, magnetite, and hematite [14]. It is not known how much simulant was produced or whether it is available for researchers in China.

Y-Mars Mudstone Analogue was developed by UK Centre for Astrobiology of the University of Edinburgh, is a mineralogical analogue of the Sheepbed mudstone analyzed by the Curiosity rover at the Yellowknife Bay location of the Gale crater [15]. The minerals were pulverized and then pressed to simulate the compaction by pressure of the Sheepbed mudstone.

OUCM-1 and -2 (Open University Contemporary Mars); OUEB-1 and -2 (Open University Early Basaltic); OUHR-1 and -2 (Open University Haematite-rich), are simulants that replicate specific Mars terrains based on data from the Curiosity rover [16]. They are chemically accurate with a specific focus on the ratios Fe^{2+}/Fe^{3+}, but they are not mineralogically accurate. The -1 designation is for standard simulants and the -2 designation is for those with modified Fe^{2+} concentrations.

P-MRS (Phyllosilicatic Mars Regolith Simulant) and S-MRS (Sulfatic Mars Regolith Simulant) are two simulants made by the German Aerospace Center DLR, used to specifically test the Raman laser spectrometer (RLS) on the ExoMars rover and its ability to identify organic substances and minerals [17]. The materials were crushed and mixed, then sieved into a fraction <1 mm in size for experiments with cyanobacteria.

According to reports from the CSM Planetary Simulant Database, a database of planetary simulants maintained by the Colorado School of Mines, the website for educational purposes, The Martian Garden, sells for researchers, hobbyists and teachers martian regolith based on the standard MMS simulant (Mojave Mars Simulant) produced by JPL Jet Propulsion Laboratory with designations MMS-1 and MMS-2, but it is actually altered red ash containing iron and magnesium oxide, unspecified sulfates, and other phases to eliminate discrepancies with the mass content of chemical elements (the developers of MMS were not consulted by The Martian Garden). On the package is listed a table confusingly indicating the percentage of minerals and the weight percentage of oxides added to 100%.

MBas (Mars Basalt), MSul (Mars Sulfate-rich), MPSmec (Mars Phyllosilicatesmectite), MPChl (Mars Phyllosilicate-illite/chlorite) and MCarb (Mars Carbonaterich), are simulants produced at the Geology Laboratory of the Universityof Georgia and used in various plant growth experiments to examinesalinity, toxicity and bioavailability of nutrients [18]. MBas and MSul are regolith simulants, while the others are rock simulants, constructed from from natural or commercial materials, selected on the basis of their composition and compatibility with data obtained from rover and orbiter missions.

WNMS (Winder Nai Mars Simulant), a multipurpose simulant designed by the University of Engineering and Technology in Lahore, Pakistan, using basalt dust from a deposit near the city of Winder in Pakistan [19]. Since it is of recent, it has not yet been used for astrobiology experiments.

The Exolith Lab site is a nonprofit extension of the Center for Lunar & Asteroid Surface Science (CLASS) at the University of Central Florida, is concerned with reproducing regolith simulants and applied research, making available a database of planetary simulants, including their specifications and MSDSs. Mineral recipes are open source and can be modified as desired.

Simulants must be handled in accordance with the directions in the relevant MSDSs because of the presence of fine dust and crystalline silica. None of the simulants reviewed contain perchlorates; some contain sulfuric anhydride and sulfates.

Fig 1: Comparison images between Martian simulants (photo: CLASS Exolith Lab and CSM Planetary Simulant Database, [18, 19].

2. The model

2.1 Inhospitable characteristics of the martian environment.

Although Mars is potentially suitable for plant cultivation, its environmental conditions must be addressed to achieve food production [20]: a lower gravity (0.38 g) than on Earth, an atmosphere rarefied, an average temperature of -63 °C, water scarcity, continuous exposure to radiation and ionizing particles, and a geological evolution that has created toxic conditions, make the red planet inhospitable.

Mars began to lose water about 3.7 billion years ago, throughout the Hesperian period, characterized by multiple alternating phases of higher and lower humidity that may have favored the binding of water to rocks, until the final evaporation of water about 3 billion years ago [21]. It is estimated that the presence of hydrate minerals varies with latitude [22]: 3-5% by weight, at low latitudes, equatorial and tropical (30°); ~13% by weight, at high northern latitudes; ~8% by weight, for southern high latitudes. This means that water is no longer available for the planet's hydrological cycle.

This was all due to the disruption of the magnetic field that once protected the planet from solar radiation, consequently causing the progressive rarefaction of the atmosphere [23-25], partly due to low gravity [26, 27]. The martian atmospheric pressure is less than 1% compared to that of Earth, which means that water cannot exist in the liquid state unless the pressure rises or the temperature falls. In depressions deepest, the atmospheric pressure on Mars turns out to be about 0.5 to 1 kPa [28], while on Earth the average value is 101 kPa. Figure 2 shows the state diagram of water as a function of temperature and pressure: on Earth, large amounts of water can be found in both liquid and solid, whereas on Mars the low pressure makes liquid water unstable, allowing its existence as ice or sublimated directly into vapor water [29].

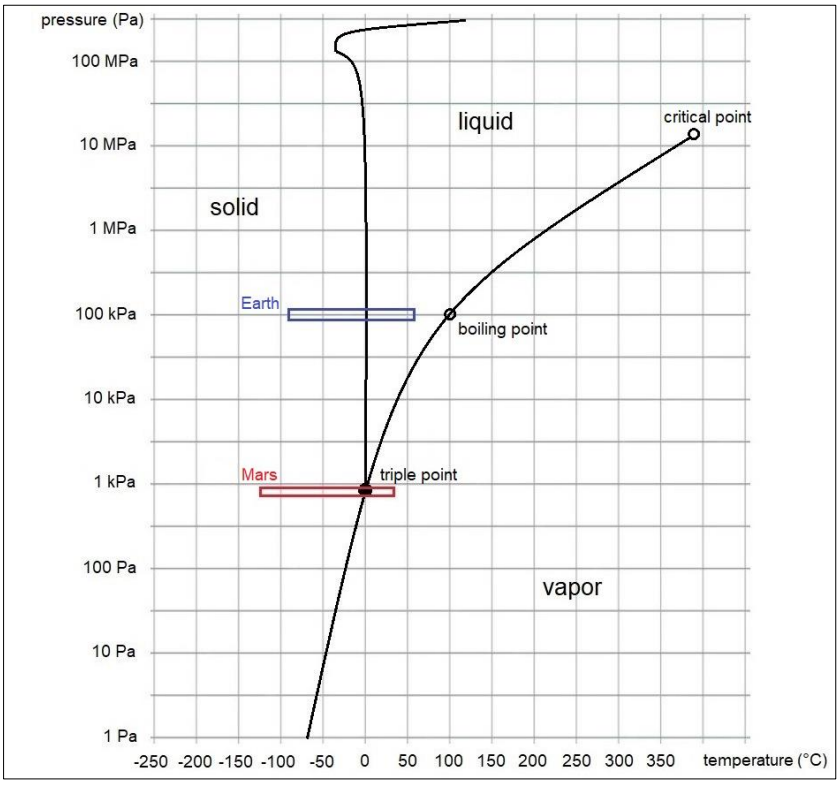

Fig 2: Water state diagram.

Table 1: Composition of the atmosphere of Mars and Earth. 1 ppm is equivalent to 0.0001%.

	Mars	Earth
CO_2	95.32%	0.03%
N_2	2.70%	78.1%
Ar	1.60%	0.93%
O_2	0.13%	20.95%
CO	0.08%	-
H_2O	210 ppm	0.33%
NO	100 ppm	-
Ne	2.5 ppm	1.82 ppm
Kr	0.3 ppm	11.4 ppm
Xe	0.08 ppm	8.7 ppm

The presence of perchlorates ClO_4^-, with concentrations from 0.4 to 0.6% [37], does not allow plant growth to be sustained or could render inedible plants, also promoting the uptake of metals in doses harmful to humans [38, 39].

2.2 Characteristics favorable for growing vegetables on Mars

To assess the feasibility of growing plants on Mars, it is essential to consider several features of the martian environment: presence of liquid water, a source of energy for photosynthesis, presence of nutrients, and a chemically and physically favorable environment (pH, redox potential Eh, salinity, grain size, water retention capacity) [40].

Presence of water

First, the presence of water is essential because it is a basic requirement for plant life. Missions to Mars have found that water is not completely absent, but occurs in different forms than on Earth, mainly as ice (Figure 3), trapped in minerals in the planet's crust (Figure 4) and probably as liquid salt water [41-51].

There are several strategies under discussion to obtain water on Mars, the most efficient is extraction from frozen reserves: a system is proposed for the extraction and purification of water from underground ice using a drill tube with a heated tip and equipped with a sealing mechanism [52] to prevent sublimation of ice due to low pressure (Figure 2).

A more complex process involves the extraction of water from clay minerals, such as smectite [53], or, much less efficient are: the collection, by heating, of water adsorbed or bound to regolith minerals in a granular [44], or the collection of water from atmospheric moisture: every night, water from the liquid salt solutions that collect on the martian surface, during the day is transformed into vapor [54] that can be used by the astronauts to produce drinking water; however, the size, energy required, the space occupied and the technical complexity of the required system make the approach currently impractical for use on Mars [55].

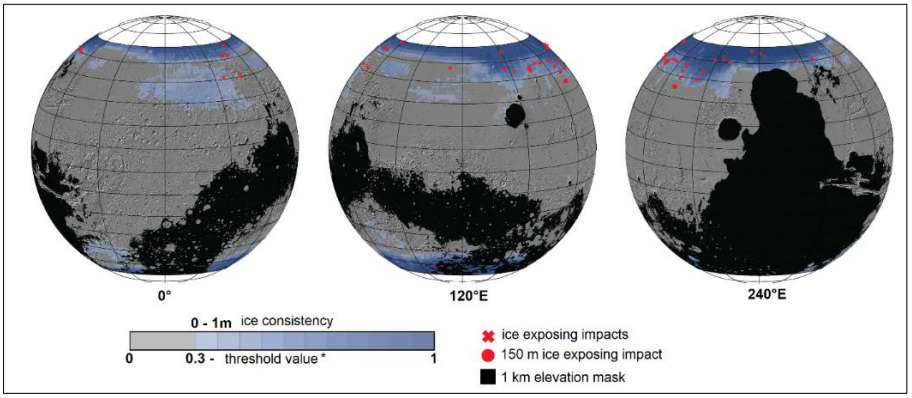

Fig 3: Map of the probable distribution of water ice buried within one meter obtained from the Subsurface Water Ice Mapping (SWIM) project, which uses data from three NASA orbital missions. Also shown are the asteroid impacts that expose surface ice, showing its the actual presence (source: NASA/JPL-Caltech/PSI).

In any case, to reduce external water inputs, plants should be grown in presaturated environments, protected from radiation and designed to capture and recycle water transpired by the plants, using greenhouses [56-58], in caves excavated from lava [59], or in underground tunnels [60].

With a gravity level equal to that of Mars, water flows more slowly into the soil, thus reducing its supply and providing a greater availability a of nutrient uptake. Plants trigger an adaptive to the new environment, the roots show an obvious gravitropism (a process that modulates the orientation of growth, visually detectable in the form of a direction defined according to the gravity vector) and, as a result, a balanced distribution of plant growth hormone (auxin) throughout the root, especially when red photostimulation is provided [30].

Energy for photosynthesis

Although Mars receives less sunlight than Earth, this is still sufficient to support plant growth by photosynthesis, but the thin CO_2 atmosphere allows UV light, with $190 < \lambda < 300$ nm, to form radicals free oxidants that rapidly decompose any organic material on the surface [29], a problem that can be solved by artificially illuminated greenhouses.

Availability of nutrients

The elements essential for life, known as CHNOPS (Carbon, Hydrogen, Nitrogen, Oxygen, Phosphorus and Sulfur), must be available in the regolith to nourish plants, especially of C, H and O, obtained from photosynthesis, elements of which which are composed of 90 to 99% of the plant body, the remainder being made up by the mineral component.

Based on data from satellites and rovers [61], the martian regolith appears to contain all the major elements (macroelements: carbon, hydrogen, oxygen, nitrogen, phosphorus, potassium, calcium, magnesium, sulfur) and many of the minor elements (trace elements: iron, manganese, zinc, copper, boron, and molybdenum) in quantities sufficient to support healthy plant growth, but it lacks organic matter (e.g., the optimal content for vegetables is between 5 and 8%) and biotic activity.

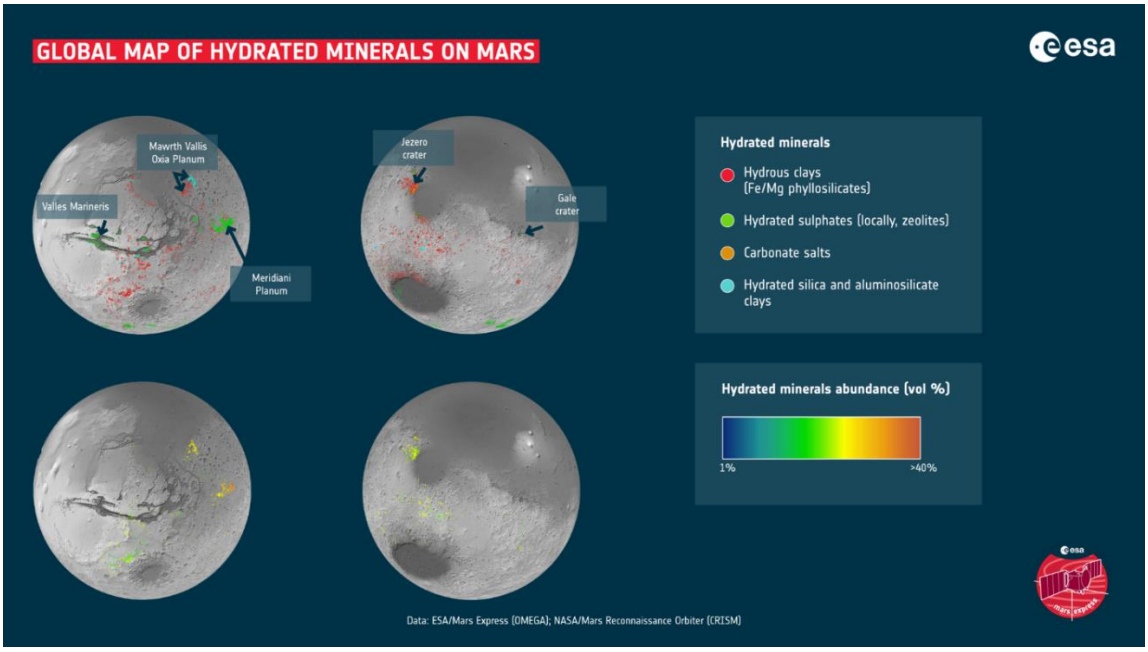

Fig 4: Global map of hydrate minerals on Mars.

Shown are the locations and abundances of hydrate minerals (clays and salts) derived from the chemical alteration of rocks due to the action of water (Source: Esa/Mars Express (OMEGA) and Nasa/Mars Reconnaissance Orbiter (CRISM)).

Then there are other elements absorbed by plants, in very small amounts, which do not meet the criterion of essentiality such as silicon, sodium, aluminum and cobalt.

ALL elements are essential for plant growth and development and cannot be substituted for each other; even if one nutrient is lacking, the plant cannot take root. Although many elements are present in quantities sufficient, they may not be present in a bioavailable form resulting in nutritional disorders (growth deformation, flowering disorders and ripening).

A high concentration of a single element may favor or limit the uptake of another element, and despite having sufficient quantities in the soil of the individual elements, the plant fails to absorb them. In Figure 5, the interaction between the elements is represented with the Mulder's diagram [62].

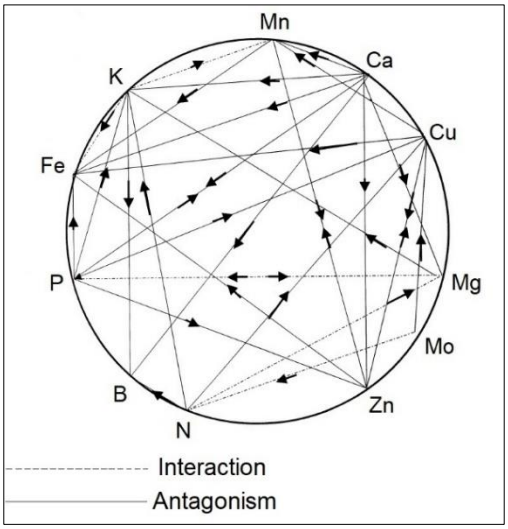

Fig 5: Mulder's diagram.

The dotted line of interaction occurs when the high level of a particular nutrient increases the plant's demand for another nutrient. The solid line of antagonism occurs when the high level of a particular nutrient hinders the availability and uptake of another nutrient.

The presence of carbonates in the regolith and an atmosphere mainly formed by CO_2, signify abundant sources of inorganic carbon [40].

Hydrogen production is achieved through the electrolysis of the molecule H_2O, or by the serpentinization process of iron-rich olivine (hortonolite) [63], or from iron-rich clay minerals through reactions redox [64].

Atmospheric nitrogen N_2 occurs in a form that does not easily react with other molecules, it needs to be dissociated and react with other atoms to form nitrate salts NO_3^- and ammonium salts NH_4^+. Unlike Earth, there are no organisms on Mars that are able to fix atmospheric nitrogen in order to be absorbed by plants, but it may have been fixed abiotically through mechanisms such as heat shock caused by falling meteorites and lightning [65] and by the interaction of light with the surface that could give the possibility of the existence of a nitrogen cycle, in which N_2 is continuously converted to NO_3^- and then released back into the atmosphere [66]. It is estimated that the amount of nitrate varies from 70 to 1100 ppm [67].

The martian atmosphere (Table 2) does not allow aerobic respiration because of the low oxygen content. There are several strategies under study to obtain O_2: production by electrolysis of CO_2 [37], exploiting deposits of perchlorate salts as sources of oxygen [68], using of minerals on the planet as catalysts to accelerate the chemical reactions chemicals involved in oxygen extraction [69]. One economic system that could be useful in supporting germination and plant growth is based on a lightly cross-linked polyacrylate that will swells and donates oxygen when hydrated under a CO_2 atmosphere [70].

The fraction of phosphorus available to plants, by convention expressed in terms of phosphorus pentoxide P_2O_5, is represented by soluble phosphorus and exchangeable phosphorus. On Mars, the abundance of phosphorus is about

10 times greater than on Earth, but it is in the form of non-assimilable mineral phosphorus, that is, incorporated into the crystal lattices of apatites and whose mobility occurs through the dissolution of these minerals in acidic environments [71, 72].

Sulfur to be absorbed by plants must occur in the form of sulfates SO_4^{2-}. On Mars they have been found predominantly in the form of $MgSO_4$ with a small amount of $CaSO_4$ [73].

The hydrogen potential and the oxidation-reduction potential

The chemical evolution of soils is determined by proton transfer in the acid-base reactions and by electron transfer in oxidation-reduction reactions. The hydrogen potential *pH* measures the concentration of hydrogen ions (protons) of a substance. The oxidation-reduction potential E_h (expressed in mV) measures the tendency of a substance to acquire electrons (oxidation) or to give up electrons (reduction).

pH and E_h affect the availability of nutrients (Figures 6 and 7) and the activity of microorganisms (bacteria and fungi) useful to plants for the degradation of organic matter, for nitrogen fixation, for phosphate solubilization and for the production of plant hormones.

The *pH* of the surface of Mars is not uniform, varying from 6.8 to 8.3, this depends on the composition of the minerals present: some are indicators of acidic and oxidizing, others of alkaline and reducing environments [75]. For most crops, the ideal soil has $6 < pH < 7$ and $+400 < E_h < +450$ mV (Figure 7). The Phoenix lander measured an oxidation-reduction potential $E_h = +253 \pm 6$ mV and a pH = 7.7±0.1 at 8.4 °C [76], values that are out of the range of habitable soils [77] and in which some bacteria and fungi useful to plants [78].

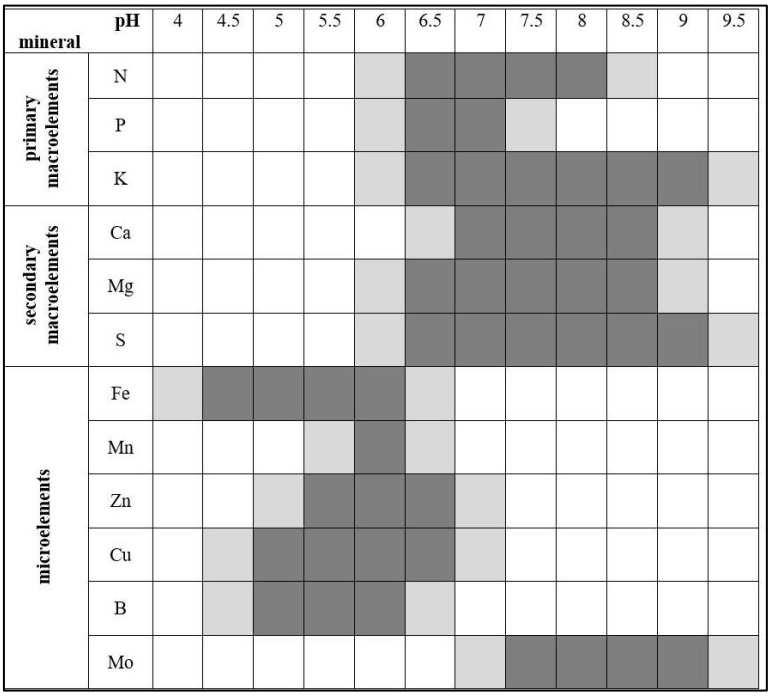

Fig 6: *pH* and element availability.

pH is defined as a measurement scale used to express the acidic (0-6) or alkaline (8-14) of solutions. *pH* measures the amount of hydrogen atoms that carry positive charges; the higher the concentration of hydrogen ions, the more acidic the sample; the lower the concentration of hydrogen ions, the more basic or alkaline a sample is. The *pH* affects the availability of the elements: Dark gray, light gray, and white indicate the *pH* values, respectively optimal, acceptable and zero for the uptake of the elements.

Salinity

E_c electrical conductivity is the reciprocal of electrical resistivity and expresses the measure (mS/cm) of how easily a material allows the passage of electric current, this is proportional to the concentration of ions in solution; the more salts there are, the more current passes. A soil is considered saline when $E_c > 4$ mS/cm, this causes slower plant growth and nutritional imbalances.

The Phoenix lander measured an average conductivity of ~ 1.4 ± 0.5 mS/cm for the 1:25 soil/solution mixture [73], a value generally considered acceptable for many crops.

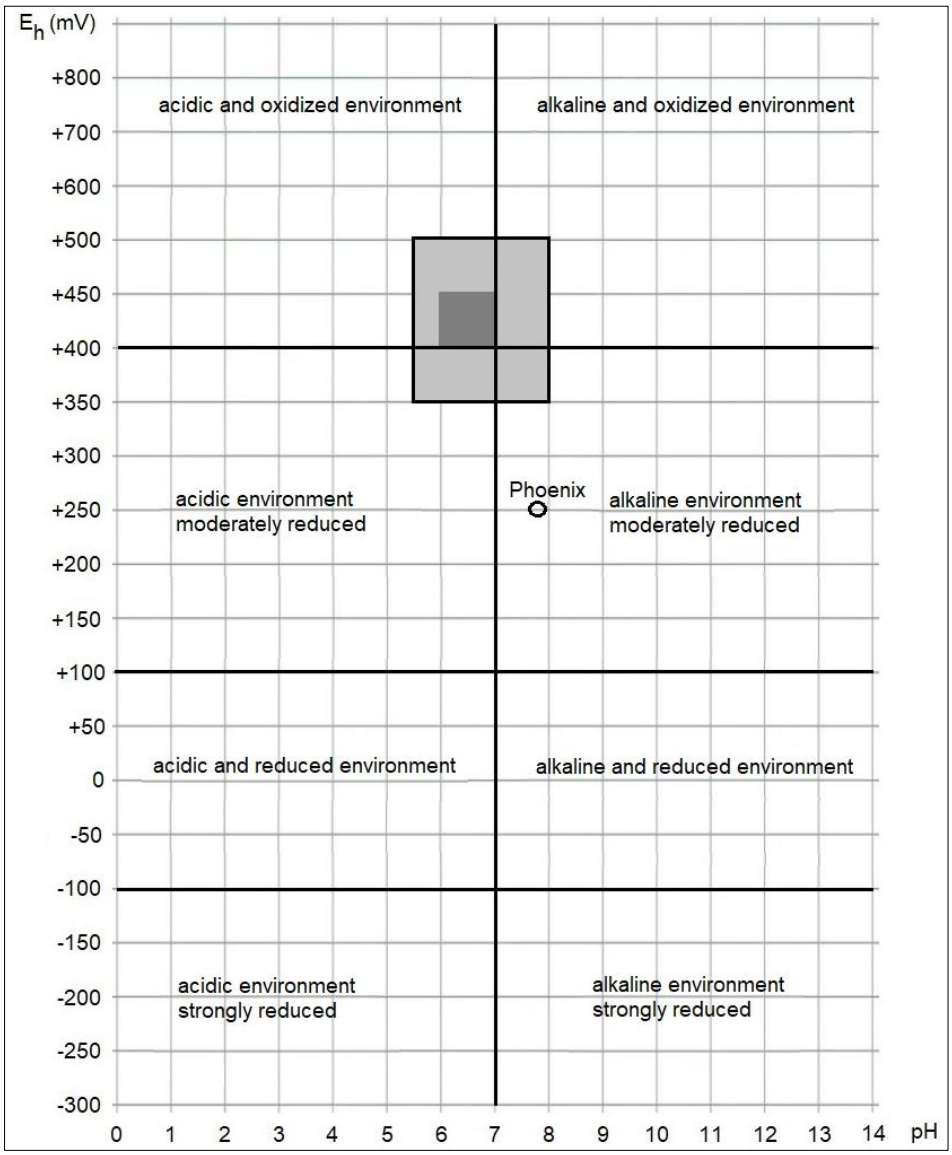

Fig 7: Pourbaix's diagram.

The redox potential is closely related to the degree of aeration, i.e., the oxygen availability of the soil. Oxygen is the strongest oxidizing agent, hydrogen is the strongest reducing agent. The area in light gray is generally considered favorable for the growth plants, while the area in dark gray indicates environmental conditions that are optimal.
The circle indicates the measurement made by the Phoenix lander.

Structure of the regolith

The size of local and regional basaltic materials of the outermost layer of the surface, composed of the regolith (heterogeneous set of sediments, dust and fragments), are the result of a combination of geological processes of physical events (meteorite and comet impacts, volcanism, wind and water) and chemical reactions (aqueous alteration, oxidation). The grain size of Mars regolith (Table 2) is composed of particle sizes clay less than 0.004 mm (between 15 and 25 percent by weight) and a combination of silt and sand less than 2 mm in size (between 75 and 85 percent by weight). The finest fraction, i.e., dust (1-3 μm), is suspended by wind and is transported on regional and global scales and remixed with the surface [61]. However, these estimates may vary locally.

The presence of clay particles (15-25% by weight) indicates that the regolith of Mars has a significant fine component. This could affect the mechanical properties of the soil, such as permeability to water and air, and the water retention capacity. Clay particles tend to retain nutrients better than particles larger ones. Therefore, if there were nutrients present, they could be more readily available for possible life forms or plant growth. The presence of a combination of silt and sand (75-85% by weight) suggests that the soil could be relatively easy to work with. However, the presence of clay particles could make the soil more difficult to work when it is wet.

Table 2: Particle size distribution [74] of the surface of Mars. Martian regolith is the unconsolidated surface material covering the rocky solid. Dust is the finer fraction that is suspended by the wind and remixed with the surface on a global scale.

Grain size class	Size (diameter in mm)	weight percentage (wt%)
silt and fine sand	< 2	75 − 85
clay	< 0.004	15 − 25
powder	0.001 − 0.003	−

3 Materials and Methods

Characteristics of the MSP-1 simulant for plant cultivation

A simulant, named MSP-1 (Mars Simulant for Plants), Figure 8, with mineralogical characteristics that aim to be compatible with those of martian regolith based on the results obtained from analyses performed by orbital probes, landers and rovers [61].

Thanks to the information on the content of the commercially found rock powders, it was possible to compose the simulant with percentage ranges of the various minerals compatible with those of martian regolith. The MSP-1 simulant contains mainly basalt, consisting of plagioclase feldspars (~ 30%), feldspathoids (~ 50%), olivine, pyroxenes, and augite (~ 10%), phyllosilicates (~ 4%), iron oxides (~ 2%), sulfates and carbonates (less than 1%).

A rough estimate of the following chemical and physics of the simulant:

hydrogen potential $pH_{MSP-1} \simeq 8.50$ (20 °C).

oxidation-reduction potential $E_{h,MSP-1} \simeq -90$ mV (20 °C).

electrical conductivity $E_{c,MSP-1} \simeq 0.9$ mS/cm

apparent density $\rho_{a,MSP-1} \simeq 1.23$ g/cm^3.

porosity $P_{MSP-1} \simeq 28.5\%$.

water retention capacity (total humidity) $U_{t\%,MSP-1} \simeq 28\%$.

Table 3

MSP-1 Grain size class	Size (diameter in mm)	weight percentage (wt%)
very fine gravel and coarse sand	< 3	14
fine and very fine sand	< 0.2	80
silt and clay	< 0.00625	6

Earth soil

A terrestrial soil sample was used (Figure 8) to have a comparison with the results obtained with the simulant, in order to have a more complete view of the challenges and potential solutions for growing plants on Mars. The soil contains mainly chlorides (751 mg/l Cl^-), bicarbonates (342 mg/l HCO_3^-), sulfates (185 mg/l SO_4^{2-}), nitrates (11.1 mg/l NO_3^-), phosphates (less than 0.20 mg PO_4^{3-}), total iron (0.16 mg/l).

The chemical and physical properties are:

hydrogen potential $pH_{soil} \simeq 7.27$ (at 20 °C)

oxidation-reduction potential $E_{h,soil} \simeq 32$ mV

electrical conductivity $E_{c,soil} \simeq 2.51$ mS/cm

bulk density $\rho_{a,soil} \simeq 1.28$ g/cm^3

porosity $P_{soil} \simeq 6.3\%$.

water retention capacity (total moisture) $U_{t\%,soil} \simeq 30\%$.

Table 4

Soil Grain size class	Size (diameter in mm)	weight percentage (wt%)
fine and very fine sand	< 0.2	70
silt	< 0.00625	8
clay	< 0.0004	22

The soil was placed in pots with natural environment and lighting, varying temperatures in the range 4 - 20 °C, with 40 total seeds and watering regularly to maintain constant humidity, without adding fertilizer.

a) MSP-1 Mars Simulant for Plants b) earth soil

Fig 8

Selection of vegetables

In selecting the type of plants to be grown, preference should be given to those characterized by short crop cycle, small size, disease resistance, high productivity, high energy and/or protein and/or antioxidant content. Have been carried out germination and growth trials of plants that are normally part of the food diet: romaine lettuce (*Lactuca sativa L.*), turnip (*Brassica rapa var. cymosa*), radish (*Raphanus sativus L.*), pepper (*Capsicum annuum*), chard (*Beta vulgaris vulgaris*), spinach (*Spinacia oleracea*), tomato (*Solanum Iycopersicum*), bean (*Phaseolus vulgaris*), pea (*Pisum sativum*), lentil (*Lens culinaris)*, chickpea (*Cicer arietinum*) and broad bean (*Vicia faba maior*).

Among all these plants, those that gave rapid development were leguminous plants, one in particular, the broad bean (*Vicia faba maior*), was found to be the most suitable one for the detection of various growth parameters.

Characteristics of Vicia faba maior

Broad bean belongs to Class: *Dicotyledonae*, Order: *Leguminosae*, Family: *Papilionaceae*, Species: *Vicia faba maior*.

As a food plant, it produces large and long pods with large and flattened, which is why it has been the main food protein base of many populations in the Mediterranean and Middle Eastern areas since ancient times.

Is a fast-growing, upright, glabrous annual herbaceous plant, gray-green in color, with indeterminate development. The root is taproot capable of deepening up to 90 cm, rich in voluminous tubercles that effect, like all leguminous plants, the fixation of atmospheric nitrogen thanks to the symbiosis it establishes with certain bacteria. The stems are erect, fistulous, quadrangular, tall up to 1.50 meters, unbranched. The leaves are alternate, paripinnate, composed of two or three pairs of entire elliptic sessile leaflets. The flowers arise at the axil of the middle and upper leaves of the stem, are single or clustered and are rather showy.

It adapts well to heavy, loamy, clay-limestone soils and does not do well in loose, humus-poor, organic ones prone to waterlogging. The optimal soil *pH* conditions are close to neutrality but tolerates well *pH* values as low as 8.4. In contrast, soils are always harmful acidic with $pH < 6$.

Ideal growing temperatures range from 15 to 18 °C. This plant withstands a minimum temperature of 4 °C and a maximum temperature of 23 °C. The broad bean is among the moderately salinity-sensitive species, with a threshold of 1.6 mS/cm, with total loss of production at 12 mS/cm.

Setting up the growth chamber

For plant growth, a walled growth chamber was constructed with insulated with polystyrene panels, covered internally

with a reflective film, equipped with temperature and humidity sensors and two air intakes, lower and upper, for recycling. On the support surface (90 x 40 cm) was placed a 50 W heating cable of 6 m length, connected to the thermostat to maintain the temperature around 20 °C. The air used was ambient air. The inspection window was constructed with double layers of polyethylene sheets bubbles, sheets of reflective film, and discs of supermagnets attached at the edges so as to adhere perfectly to the metal frame of the chamber to ensure thermal insulation (Figure 9).

Fig 9: Growth chamber with thermally insulated panels and covered with film reflective.

For artificial lighting, four 20 W LED tubes were used. full spectrum, with 11% red light (λ = 660 nm), 67% yellow light (λ = 580 nm) and 22% blue light (λ = 460 nm), attached with adjustable string ratchets to be able to vary the distance from the plants. At an average distance of 20 cm, of an
LED tube from the top of the plants, the photon flux density (indicated by the manufacturer) for photosynthesis is ~ 102 µmol/m^2/s.

Setting up the pots with pure simulant

Forty jars were used, with paper filter at the bottom to prevent the escape of material, each filled with 300 g of simulant, sterilized at 120 °C and arranged in trays to collect excess water (Figure 10).

For each jar, a fava bean seed was inserted vertically with the hilum (the point of attachment to the broad bean pod) facing downward and watered with 20 g of demineralized water to mimic Mars water, obtained through the various processes mentioned earlier and also to avoid administering the nutrients present in tap water.

For all simulant handling operations, up to the first watering for planting, a mask was used for protection from the dust.

From sowing until germination, the frequency of watering was every two or three days depending on the evaporation rate; every other day until the opening of the first leaves and finally once a day until the end of the experiment. Monthly water consumption was about liters. From the beginning of watering, the air humidity values varied between 60 and 80%. Artificial lighting was activated from the time the seedlings took upright position, for a day:night cycle of 16:8.

Fig 10: Growth chamber with the vessels filled with simulant.

Statistical Analysis

To determine whether there were significant differences in growth parameters (height and leaf area) between plants grown in the martian simulant and in terrestrial soil, a statistical test called the paired-sample t-test was used. This method is particularly suitable for comparing two distinct conditions, such as the martian simulant and terrestrial soil, when the same parameter is measured on the same samples (the plants) over the same period of time.

A significant difference would suggest that the substrate has a measurable effect on plant growth, while a lack of significance would imply that the observed variations could be due to chance or natural variability. Measurements for parameters such as plant height and leaf area were recorded daily for plants grown in both conditions. Each pair of measurements represents values collected on the same day for the same sample.

Statistical analysis was performed as follows:

- Calculation of the difference: for each day of observation, the difference between the values measured in the simulant and in the terrestrial soil was calculated.
- Mean of differences: the mean of these differences was calculated to estimate the average effect using the formula: $\mu = \frac{\sum differences}{n}$, where n represents the number of paired observations.
- Standard deviation: the variability in differences was quantified using the standard deviation, calculated as: $\sigma = \sqrt{\frac{\sum(differences-\mu)^2}{n-1}}$.
- *t-value*: the *t-value*, which represents the magnitude of the difference between the two data sets with respect to their variability, was calculated using the formula: $t = \frac{\mu}{\sigma/\sqrt{n}}$.
- *p-value*: The *p-value* was obtained from the t-distribution using the calculated *t-value* and the degrees of freedom (n−1). This value represents the probability that the observed differences occurred by chance.

A *p-value* < 0.05 was considered statistically significant, indicating that the observed differences were unlikely to be due to chance variation. In contrast, a *p-value* ≥ 0.05 suggested that the observed differences could be attributed to chance or natural variability.

If the normality assumption required for the paired t-test was not met (i.e., the differences were not normally distributed), a non-parametric alternative, such as the Wilcoxon signed-rank test, was used. This test is robust to deviations from normality and assesses whether the median of the differences differs significantly from zero. This approach ensured a rigorous and appropriate statistical assessment of plant growth in the two substrate conditions. The normality assumption was verified by a Shapiro-Wilk test (p=0.018), and we used the Wilcoxon test in the case of plant height analysis.

4 Results

4.1 Germination

To assess germination, we counted the number of seeds that, on the tenth day after sowing, had developed roots at least half the length of the seed itself [82]. 10-day measurement was chosen because this period allows the germination capacity of seeds to be estimated within an appropriate time frame before the growth process proceeds further. Cumulative germination percentage *CGP* indicates the percentage of seeds that have germinated within these 10 days and is calculated using the following formula:

$$CGP = \left(\frac{seeds\ germinated\ in\ 10\ days}{total\ seeds}\right) \times 100 \quad (1)$$

For the MSP-1 simulant, out of a total of 40 seeds, 30 seeds germinated in the first 10 days and 1 seed never germinated, so:

$$CGP_{MSP-1} = \frac{40-10}{40} \times 100 = 75\%$$

Instead, in the terrestrial soil, germination was total, that is, all 40 seeds germinated within the tenth day, so the cumulative germination percentage is CGP_{soil} = 100%.

Figure 11 shows the germination pattern of seeds in the simulant, modeled with a logistic regression curve, which highlights the speed of germination in the different phases: slow in the initial phase, rapid between day 6 and day 10, and finally a tendency to stabilize. This type of 'S' pattern is typical of many biological processes.

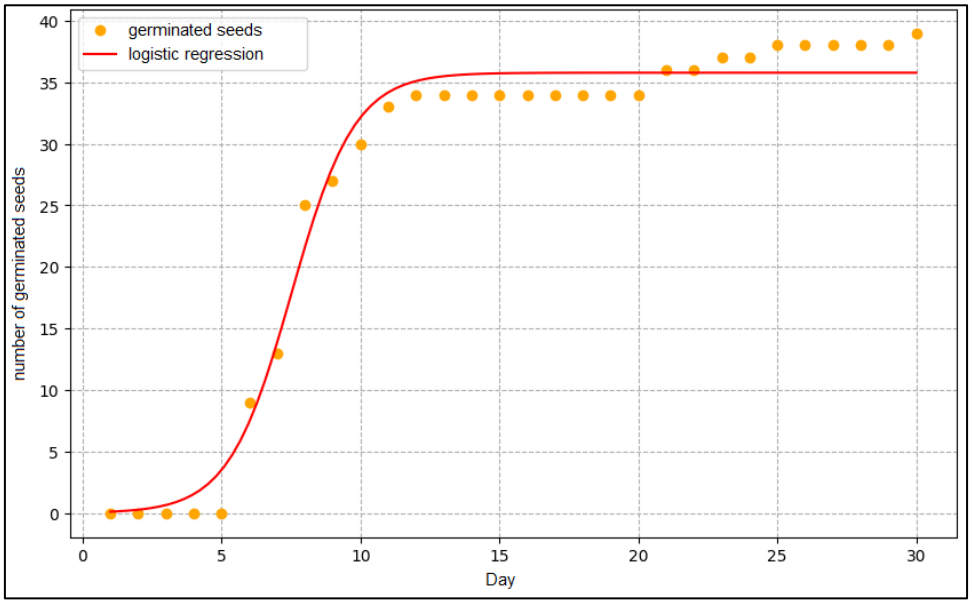

Fig 11: Germination progression over time.

The graph shows the number of seeds germinated in the martian simulant over the 30 days of the experiment. The orange dots represent the number of germinated seeds measured each day. The red line is a logistic regression curve, which describes the typical progression of a germination process, with a slow initial phase, a rapid growth phase and finally a stabilization phase. Logistic regression is a statistical tool that allows us to model the relationship between an independent variable (Time in days) and a dependent variable with limited growth (the number of germinated seeds). The initial slope of the curve indicates the speed of germination, while the tendency to flatten out indicates the maximum number of germinated seeds. The midpoint of the logistic curve, from which germination begins to slow down, is around day 7. The x-axis indicates days, the y-axis the number of germinated seeds.

4.2 Growth parameters

Plant height

Plant height was measured with a tape measure, from the point where the root meets the stem (the hypocotyl) to the upper end of the growing part (the meristematic apex). To assess growth in height, a growth index GI_h was calculated with the following formula:

$$GI_h = \frac{h_f - h_i}{h_i} \times 100 \quad (2)$$

where h_i represents the height of the plant in the initial measurement and h_f represents the height in the final measurement, both expressed in centimeters (cm), after a period of 30 days. The GI_h provides an overall view of the growth in height of the plant throughout the experiment, allowing us to compare the growth between the initial and

final phases. This value, expressed as a percentage, tells us how much the plant has grown compared to its initial height, over the 30 days of the experiment.

To identify the periods in which plant growth is fastest, a Daily Growth Index DGI_h was calculated, which represents the percentage of growth compared to the previous day. The formula for DGI_h is as follows:

$$DGI_h = \frac{h_t - h_{t-1}}{h_{t-1}} \times 100 \quad (3)$$

where h_t represents the height of the plant on the current day and h_{t-1} the height on the previous day, both expressed in centimeters.

In the martian simulant, the DGI_h was approximately 15.0%, while in the terrestrial soil it was approximately 14.0%. These values indicate that plants grown in the martian simulant had a slightly higher daily variation in height than those grown in the terrestrial soil. Additionally, to calculate the average height growth in centimeters (cm) over the entire experiment, we used the Average Daily Growth Rate $ADGR_h$, calculated with the following formula:

$$ADGR_h = \frac{h_f - h_i}{30} \quad (4)$$

where h_f and h_i are the final and initial height in centimeters, respectively. We found that the height of the plants increased by about 1.67 cm per day in the simulant and by about 1.87 cm per day in the terrestrial soil. These values allow us to have an estimate of the average daily increase in height over the entire observation period.

Table 3 summarizes the growth conditions and growth index values obtained for plants grown in the martian simulant (MSP-1) and in terrestrial soil.

Table 3: Comparison of growth conditions and growth indices for plants grown in martian simulant and terrestrial soil.

	Germination day	Lighting	Temperature °C	Humidity %	GI_h %	DGI_h %	$ADGR_h$ (cm/day)
MSP-1	6th	16 h/day	20	60 – 80	25	15.0	~ 1.67
earth soil	8th	solar cycle	4 – 16	80	28	14.0	~ 1.87

The GI_h (Growth Index) indicates the total growth of the plant as a percentage, the DGI_h (Daily Growth Index) indicates the growth as a percentage compared to the previous day, and the $ADGR_h$ (Average Daily Growth Rate) indicates the average height growth in centimeters (cm) for each day.

As shown in Table 3, plants grown in the martian simulant showed a shorter germination time (6 days) compared to terrestrial soil (8 days). In the simulant, the lighting was artificial and constant (16 hours per day), while in the terrestrial soil the normal solar cycle was exploited (in ambient conditions). The temperature was also kept constant at 20 °C in the simulant, while it was variable (4-16 °C) in the terrestrial soil. Humidity was on average lower in the simulant (60-80%), while it was 80% in the terrestrial soil. Despite different environmental conditions, the growth index GI_h values were similar (25% and 28%, respectively), showing that the total growth in height is similar in both substrates. The average daily growth rate $ADGI_h$ indicates slightly higher daily growth for plants grown in the simulant (15.0% vs. 14.0% for terrestrial soil), but the average daily increase in centimeters $ADGR_h$ is higher in terrestrial soil (1.87 cm/day) than in the simulant (1.67 cm/day). In general, it can be seen that plants grown in field soil show a more efficient height growth than those in the simulant, as indicated by the $ADGR_h$ index (1.87 cm/day vs. 1.67 cm/day), while the differences are smaller for the overall height growth rate GI_h, where it is 28% in soil vs. 25% in the simulant.

Figure 12 shows the growth pattern of the two sample plants in the martian simulant and in terrestrial soil up to the 30th day. Both parametric (t-test) and non-parametric (Wilcoxon test) analyses highlighted a statistically significant difference in height growth between the two groups ($p = 0.0022$). This result, which rejects the null hypothesis of no difference between the two groups, indicates that the plants in terrestrial soil show an average greater growth. On average, the plants in terrestrial soil are about 3.3 cm taller than those grown in the simulant, a value obtained by calculating the mean of the daily differences between the two groups.

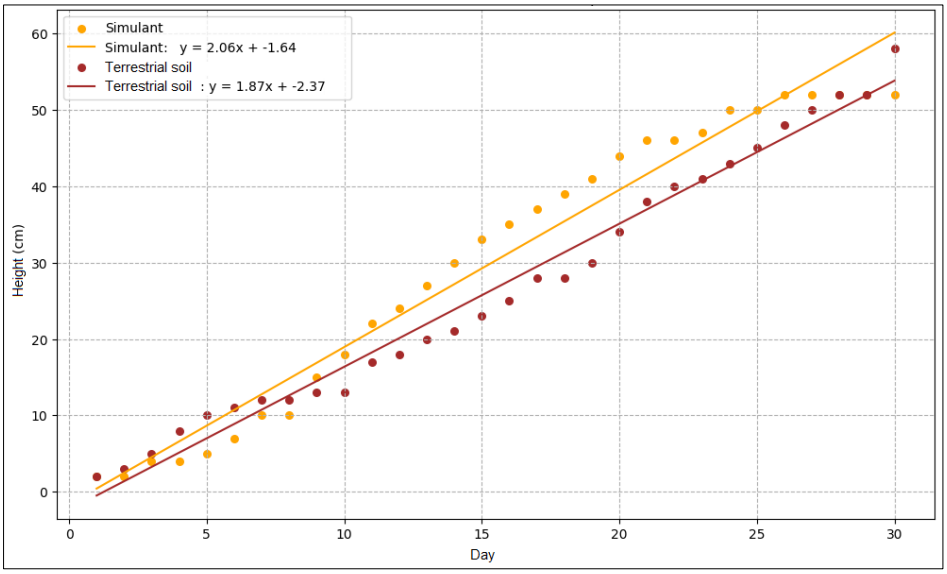

Fig 12: Plant height over time graph.

The graph shows the height in centimeters of plants in the simulant (orange line) and in the field soil (brown line) over the course of 30 days. The lines represent the growth trend over time, the equations that accompany the lines indicate the slope and the intercept, respectively. The dots represent the measurements taken day by day, and show the variability of plant growth. The x-axis indicates days, the y-axis indicates height in centimeters.

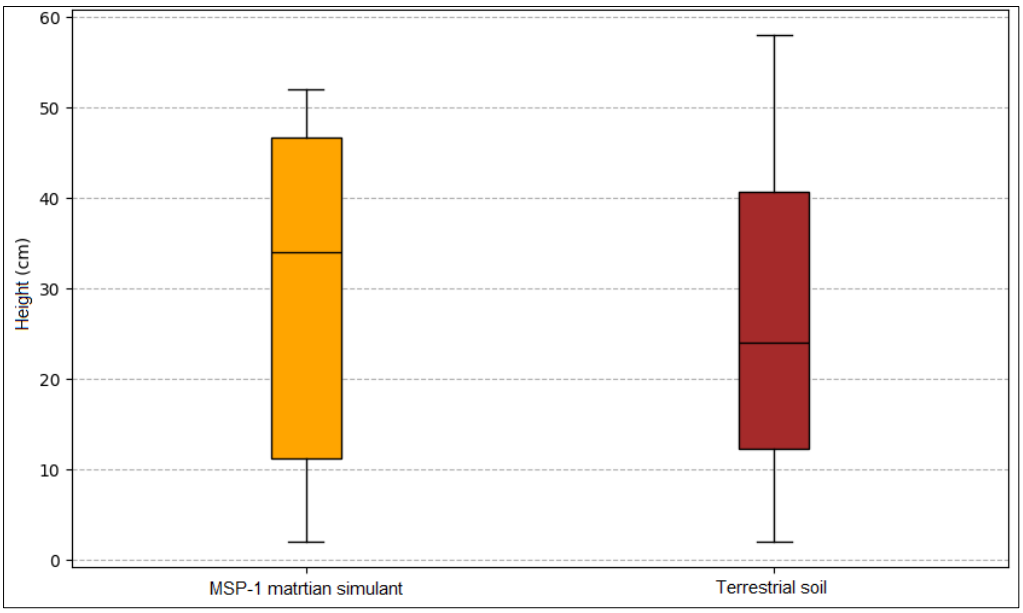

Fig 13: Distribution of plant heights at day 30.

This boxplot compares plant heights at the end of the experiment (day 30) in two different conditions: the martian simulant (left) and terrestrial soil (right). Each boxplot shows the median (the line inside the box), which indicates the central height value. The box itself represents the top 50% of the heights, sandwiched between the first and third quartiles. Whiskers extending from the box show the variability in heights, while single points outside the whiskers are outliers. The position of the boxes shows that, on average, plants in terrestrial soil are taller than those in the simulant. Additionally, the vertical width of the box in terrestrial soil indicates greater variability in heights. The y-axis indicates heights in centimeters.

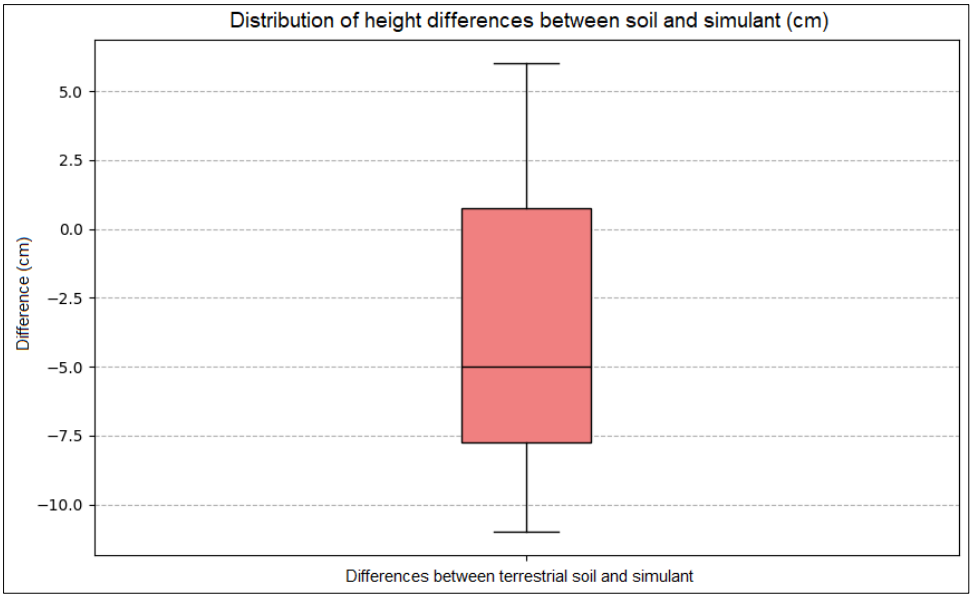

Fig 14: Distribution of height differences between terrestrial soil and martian simulant.

This boxplot shows the height differences between plants grown in terrestrial soil and in the martian simulant, calculated day by day. The differences are calculated by subtracting the height in the simulant from the height in the terrestrial soil. A negative median (the line in the box) indicates that, on average, plants in the terrestrial soil grew more than those in the simulant. The extension of the box towards negative values indicates that most of the observed differences are negative and therefore confirm greater growth in the terrestrial soil. The y-axis indicates the height differences in centimeters. These differences, as also confirmed by the statistical analysis, are significant ($p < 0.05$), and therefore not attributable to chance.

Figure 15 shows that in terrestrial soil there is a greater growth at the beginning, with a subsequent decrease, while in the simulant the growth is less variable over time.

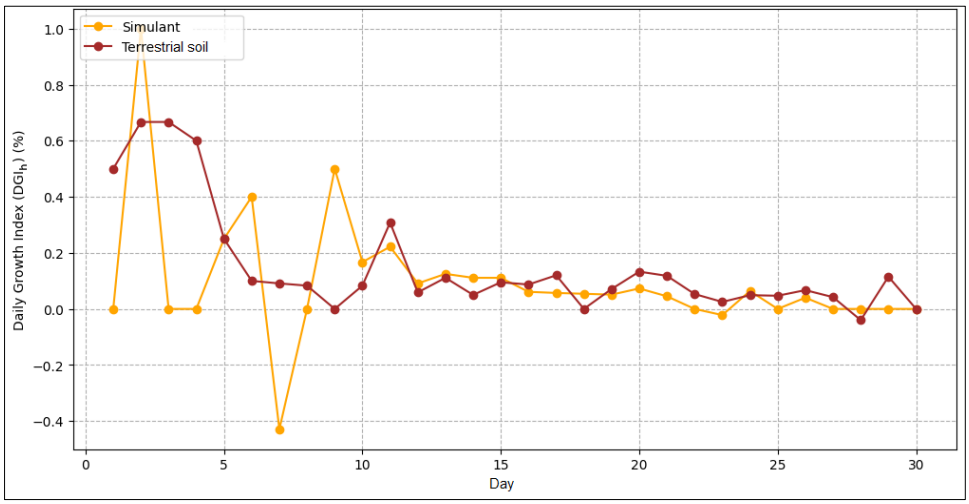

Fig 15: Daily Growth Index DGI_h trend over time.

This graph shows the Daily Growth Index DGI_h, expressed as a percentage, over time for plants grown in the martian simulant (orange line) and in terrestrial soil (brown line). The DGI_h indicates the percentage of growth in height compared to the previous day. The x-axis represents time in days and the y-axis represents DGI_h (%).

Leaf surface

Leaf area growth was measured for a leaf developed immediately after germination and for a leaf that was approximately 30 cm from the hypocotyl, the point where the root meets the stem. Leaf area was measured until the area was constant after the third measurement (taken during the last 10 days of the experiment). Leaf area was measured four times over 30 days, using the direct measurement method, which consisted of drawing the outline of the leaf on graph paper and counting its area (Figure 16a).

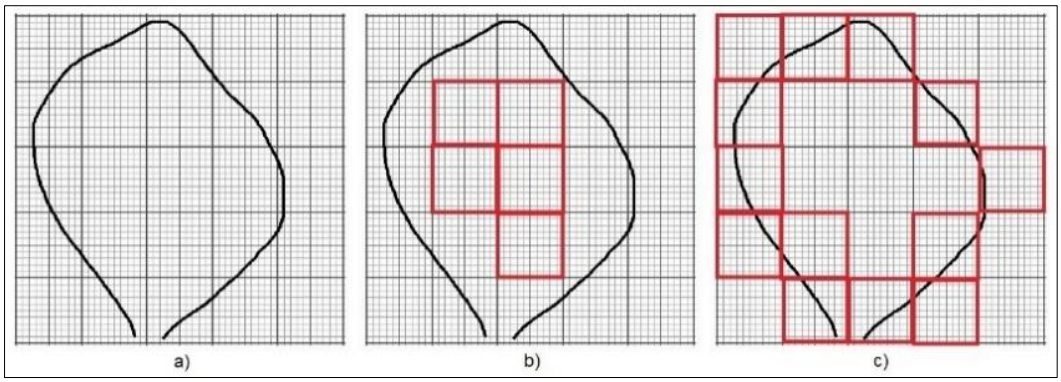

Fig 16: Method of direct measurement of leaf area.

To estimate the area, we counted the 1 cm squares entirely contained within the perimeter of the leaf (Figure 16b), obtaining an internal area S_i, expressed in mm² (multiplying the number by 100); subsequently, we counted the squares that intersected at least partially the leaf outline (Figure 16c), obtaining an external area S_e, expressed in mm² (multiplying the number by 100). The effective area of the leaf, which we call S_f, is included between the internal area and the external area $S_i < S_f < S_e$. To obtain a more precise estimate, we calculated the mean area S_m, as the arithmetic mean of S_i and S_e:

$$S_m = \frac{S_i + S_e}{2} \quad (4)$$

The absolute error on the measurement is e_a = 1 mm, while the accuracy of the measurement is given by the relative error: $\epsilon_r = \frac{e_a}{S_m} \times 100$.

In general, it can be said that a relative error of less than 5% is acceptable, while a relative error greater than 10% is excessive.

The growth index with respect to the initial leaf area is given by the formula:

$$GI_s = \frac{S_f - S_i}{S_i} \times 100 \quad (5)$$

where S_i and S_f are the first and last measurements (mm²), respectively, in the 30-day period, respectively.

To identify the periods when the leaf area is growing most rapidly, the daily growth index is calculated:

$$DGI_s = \frac{S_t - S_{t-1}}{S_{t-1}} \times 100 \quad (6)$$

where S_t represents the leaf area on the current day and S_{t-1} the leaf area on the previous day, expressed in square millimetres (mm²).

Furthermore, to calculate the average daily increase in leaf area over the entire experiment, the average daily increase in leaf area $ADGR_S$ is considered, calculated with the following formula:

$$ADGR_s = \frac{S_f - S_i}{30} \quad (7)$$

where S_f and S_i are the final and initial leaf area, expressed in square millimeters (mm²), respectively. The $ADGR_S$ indicates the amount of additional square millimeters (mm²) that the leaf area has grown, on average, each day.

Table 4 shows the growth indices of the leaf area, both for the first leaf developed after germination and for the leaf developed at a height of about 30 cm from the hypocotyl. The values of the global growth index GI_S, expressed as a percentage, show that in the martian simulant the growth of the leaf area is greater for the first leaf (75%) and less for the leaf at 30 cm (47%), while in the soil the growth is greater for the leaf at 30 cm (63%) than for the first (29%). The daily growth index *DGI*, expressed as a percentage, shows that the growth is always greater in the first leaf in the simulant, while in the soil it is greater both in the first leaf and in the leaf at 30 cm. Finally, the mean daily leaf area gain $ADGR_S$ shows that growth is greater for the 30 cm leaf, both in the simulant (about 44.4 mm²/day) and in the soil (about 83.3 mm²/day), compared to the first leaf.

These data allow to compare the growth performance of the leaf surface in two different substrates and at two different times of growth, providing an overall view of the development process.

This table summarizes leaf area growth indices, measured by the graph paper method, for both the first leaf developed after germination (*) and the leaf developed at a height of about 30 cm from the hypocotyl (**). The table compares plants grown in martian simulant (MSP-1) and terrestrial soil, and includes: type of lighting, temperature, humidity, global growth index GI_S, daily growth index DGI_S, and average daily growth rate $ADGR_S$. GI_S (Growth Index) indicates the total growth of leaf area in percentage, DGI_S (Daily Growth Index) indicates the highest percentage growth in a single day compared to the previous day, while $ADGR_S$ (Average Daily Growth Rate) indicates the average daily increase in leaf area (in mm²/day).

Table 4: Comparison of leaf area growth indices for plants grown in martian simulant and terrestrial soil.

	Lighting	Temperature °C	Humidity %	GI_S %	DGI_S %	$ADGR_S$ (mm²/day)
MSP-1	16 h/day	20	60 – 80	75 * 47 **	50 * 23.5 **	~ 33.3 * ~ 44.4 **
terrestrial soil	solar cycle	4 – 16	80	29 * 63 **	17.7 * 18.2 **	~ 27.8 * ~ 83.3 **

* values referred to the first leaf developed after gerimination; ** values referred to the leaf at 30 cm from the hypocotyl.

In Figure 17, it can be seen how the growth of the surface of the first leaf developed after germination behaves differently in the simulant and in terrestrial soil, especially in the initial phase, as highlighted by the trend lines describing this process.

To evaluate whether there were significant differences in the growth of the surface of the first leaf developed after germination, a statistical analysis was performed using a paired-sample t-test. This test is appropriate for comparing two conditions (simulant and soil) in which the data are measured on the same sample (the leaf) in the same time period.

The analysis involved the following steps: (1) the calculation of the difference between the leaf surfaces in the terrestrial soil and in the martian simulant, (2) the mean of these differences, (3) the standard deviation of the differences and (4) the calculation of the t-value and the corresponding p-value. To verify that the data followed a normal distribution, a Shapiro-Wilk test was performed, obtaining p=0.0635, for which the assumption of normality can be considered acceptable.

The results of this analysis showed a statistically significant difference in leaf area growth between the two substrates ($p < 0.00000023$), and the Shapiro-Wilk test confirms that the t-test can be used without problems. On average, the leaf area of the first leaves developed after germination in terrestrial soil was approximately 367 mm² larger than those of the martian simulant.

Figure 18 shows a boxplot summarizing the final values of leaf areas (measured on day 9) in the simulant and in the field soil. The boxplot highlights the median (the horizontal line inside the box), which represents the central value of each data group. The box itself represents the central 50% of the data, enclosed between the first and third quartiles. The whiskers extending from the box indicate the variability of the data. Instead, single points outside the whiskers represent outliers, that is, particularly extreme values.

Figure 19, instead, presents a boxplot that displays the distribution of the differences between the leaf area values (expressed in mm²) between the plants grown in the two substrates, calculated daily. The negative median indicates that the plants in the field soil, on average, have a larger leaf area than those in the simulant. The presence of whiskers and outliers indicates a greater variability of the measurements, while the extension of the box towards negative values confirms the tendency to greater values in the field soil. These boxplots, therefore, not only describe the variability of the measurements in each of the substrates, but confirm that the differences, on average, are greater in the soil than in the simulant.

Figure 20 compares the trend of leaf surface measured at 30 cm from the hypocotyl between the martian simulant and the terrestrial soil.

To assess whether there were significant differences in the growth of the leaf surface at 30 cm from the hypocotyl, a statistical analysis was performed using a paired-sample t-test. This test is appropriate for comparing two conditions (simulant and soil) in which the data are measured on the same sample (the leaf) in the same time period.

The analysis involved the following steps: (1) the calculation

of the difference between the leaf surfaces in the field soil and in the martian simulant, (2) the mean of these differences, (3) the standard deviation of the differences and (4) the calculation of the t-value and the corresponding p-value. To verify that the data followed a normal distribution, a Shapiro-Wilk test was performed, obtaining p=0.0243, which indicates a non-normal distribution and requires the use of a non-parametric test. For this reason, the Wilcoxon test for paired samples was used, which does not assume a normal distribution, and returns a p-value = 0.0039.

The results of this analysis, based on the Wilcoxon test, highlighted a statistically significant difference in the growth of the leaf surface for the leaf at 30 cm from the hypocotyl, between the two substrates (p = 0.0039). On average, the leaf surface of the leaves measured at 30 cm from the hypocotyl in terrestrial soil was found to be approximately 511 mm² greater than those of the martian simulant.

Figure 21 shows a boxplot summarizing the final leaf area values (measured on day 9) in the simulant and in the terrestrial soil, for the 30 cm leaf. The boxplot highlights the median (the horizontal line inside the box), which represents the central value of each data group. The box itself represents the 50% of the central data, enclosed between the first and third quartiles. The whiskers extending from the box indicate the variability of the data, while the single points outside the whiskers represent outliers, that is, particularly extreme values.

Figure 22, on the other hand, presents a boxplot that displays the distribution of the differences in leaf area values (expressed in mm²) between the plants grown in the two substrates, calculated daily. The positive median indicates that the plants in the terrestrial soil, on average, have a larger leaf area than those in the simulant. The presence of whiskers and outliers indicates a greater variability of the measurements, while the extension of the box towards positive values confirms the tendency towards greater values in the terrestrial soil. These boxplots, therefore, describe both the variability of the measurements in each of the substrates, and the fact that the differences, on average, are greater in the soil than in the simulant.

To visualize the daily growth trend of the leaf surface in the early stages of plant development, Figure 23 and Figure 24 respectively report the variations of the daily growth index DGI_S for the first leaf developed after germination and for the leaf 30 cm from the hypocotyl. Both graphs show, through the DGI_S index, how daily growth is discontinuous, with values that tend to alternate between peaks and zero.

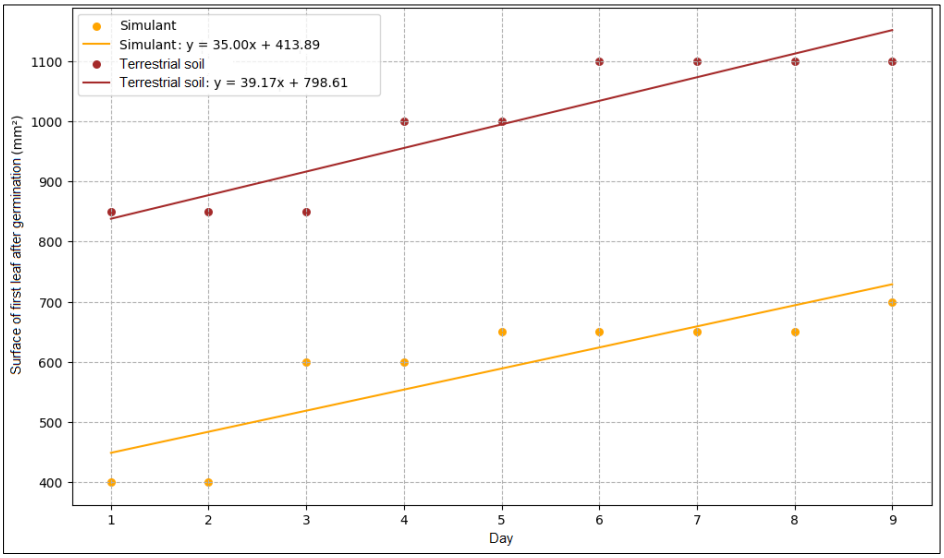

Fig 17: Plot of leaf area over time for the first leaf developed after germination.

The plot shows the leaf area in square millimeters (mm²) of the first leaf developed after germination in the martian simulant plants (orange line) and in the field soil (brown line) over the first 9 days of the experiment. The lines represent the growth trend over time, and the equations accompanying the lines indicate the slope and intercept, respectively. The points represent the values measured day by day. The x-axis indicates days, the y-axis indicates leaf area in square millimeters (mm²).

This boxplot compares the leaf areas of the first leaf developed after germination, measured on day 9 in two different growth conditions: in the martian simulant (left) and in terrestrial soil (right). Each boxplot shows the median (the horizontal line inside the box), which represents the central value of the leaf area distribution, the box (the central 50% of the data, between the first and third quartiles), the whiskers (which indicate variability), and the outliers (the single points). The position of the boxes and medians indicates that plants in terrestrial soil tend to have a larger leaf area. The y-axis indicates the leaf area in square millimeters (mm²).

This boxplot shows the distribution of leaf area differences between plants in terrestrial soil and in the martian simulant, calculated daily for the first leaf developed after germination. The difference is calculated as (Terrestrial Soil Area - Simulant Area). A positive value indicates that the plant grew more in the field soil, while a negative value indicates that it grew more in the simulant. The boxplot shows the median, the middle 50% of the data (between the first and third quartiles), the variability (the whiskers), and the outliers. The negative median indicates that, on average, the leaf area is larger in terrestrial soil. The y-axis indicates the leaf area difference in millimeters squared (mm²).

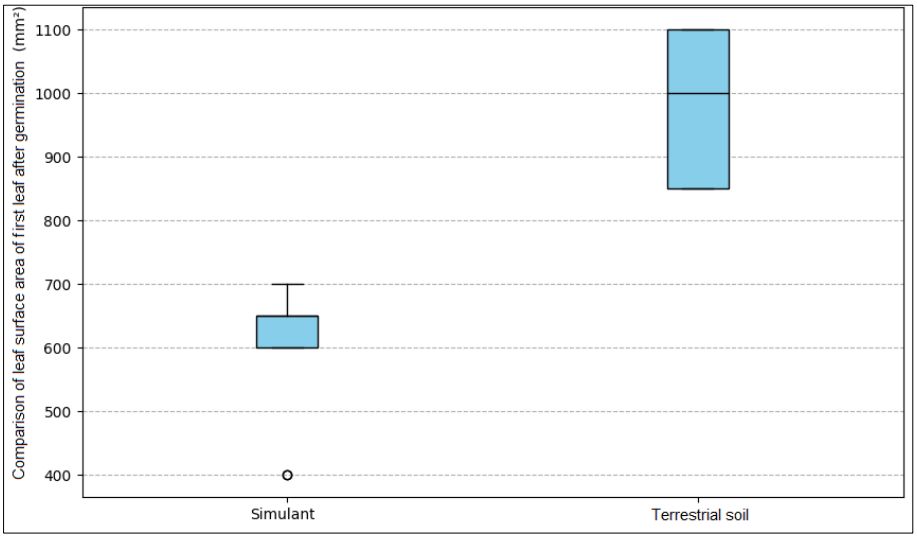

Fig 18: Final leaf area distribution (first leaf).

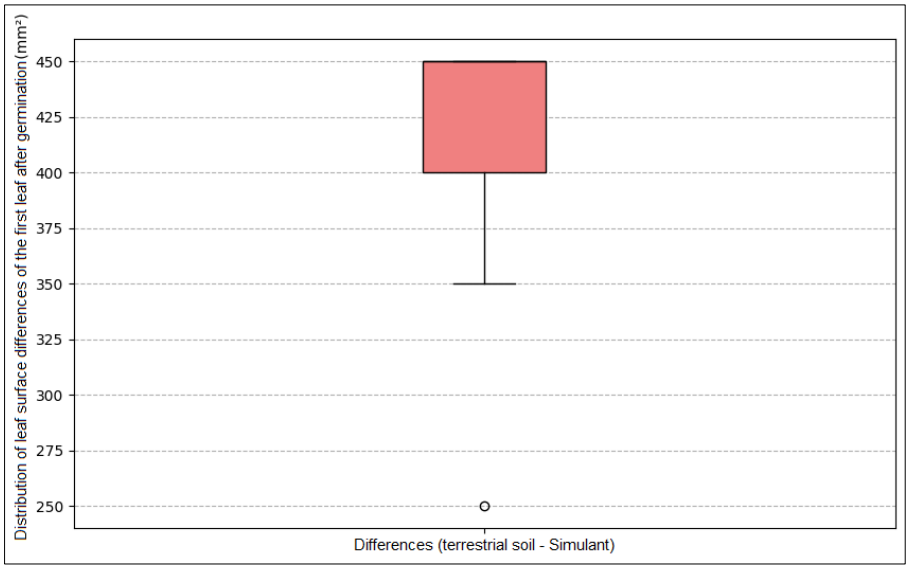

Fig 19: Distribution of leaf area differences (first leaf).

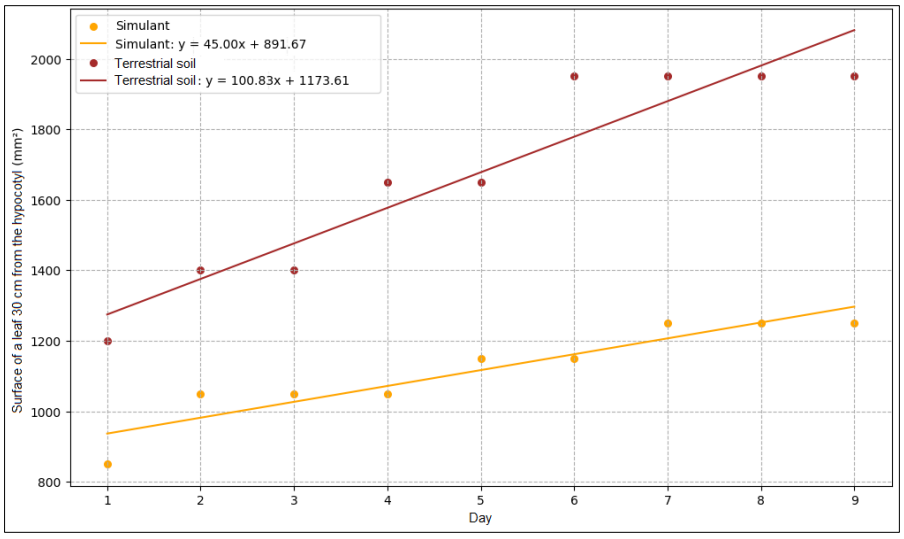

Fig 20: Leaf area trend over time (leaf 30 cm from hypocotyl).

The graph shows the trend in leaf area in square millimeters (mm^2) for leaves grown in the martian simulant (orange line) and in terrestrial soil (brown line) measured approximately 30 cm from the hypocotyl. The lines represent the growth trend over time, and the accompanying equations indicate the slope and intercept, respectively. The points represent

measurements taken day by day. The x-axis indicates time in days and the y-axis indicates leaf area in square millimeters (mm²).

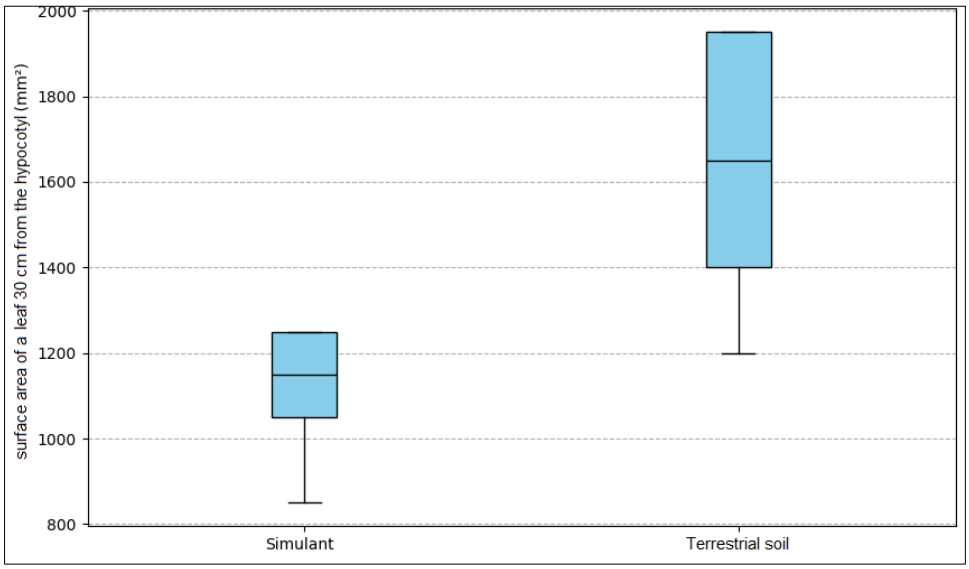

Fig 21: Final leaf area distribution (Leaf at 30 cm).

This boxplot compares the leaf areas of leaves measured at 30 cm from the hypocotyl at the end of the observation period (9 days), in two different growth conditions: in the martian simulant (left) and in terrestrial soil (right). Each boxplot shows the median (the horizontal line inside the box), which represents the central value of the leaf area distribution, the box (the central 50% of the data, between the first and third quartiles), the whiskers (which indicate variability) and the outliers (the single points). The position of the boxes and medians indicates that plants in terrestrial soil tend to have a larger leaf area. The y-axis indicates the leaf area in square millimeters (mm²).

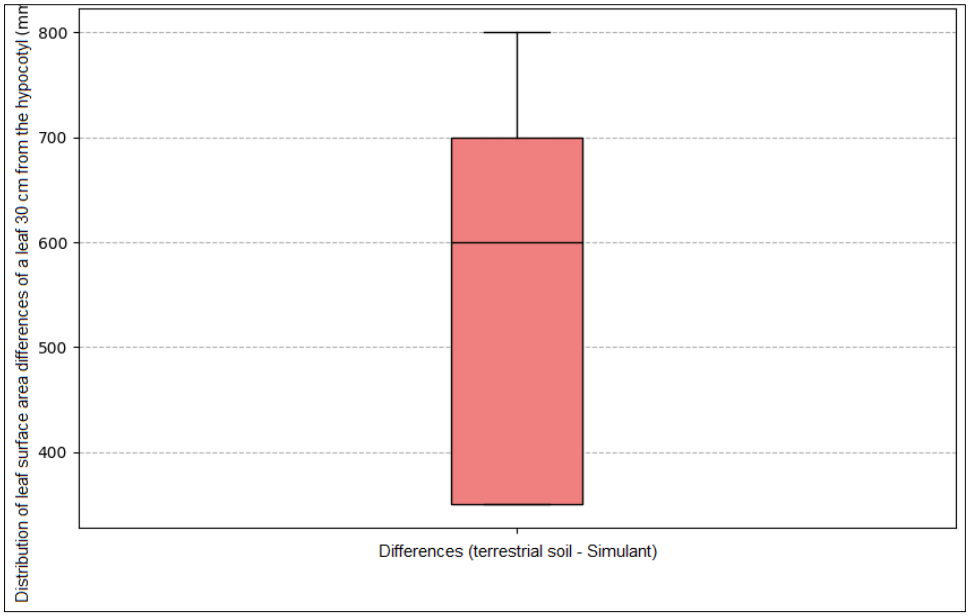

Fig 22: Distribution of leaf area differences (Leaf at 30 cm).

This boxplot shows the distribution of leaf area differences between plants in terrestrial soil and in the martian simulant, calculated daily for the leaf 30 cm from the hypocotyl. The difference is calculated as (Terrestrial soil Area - Simulant Area). A positive value indicates that the plant grew more in terrestrial soil, while a negative value indicates that it grew more in the simulant. The boxplot shows the median, the middle 50% of the data (between the first and third quartiles), the variability (the whiskers), and the outliers. The positive median indicates that, on average, the leaf area is larger in the field soil. The y-axis indicates the leaf area difference in millimeters squared (mm²).

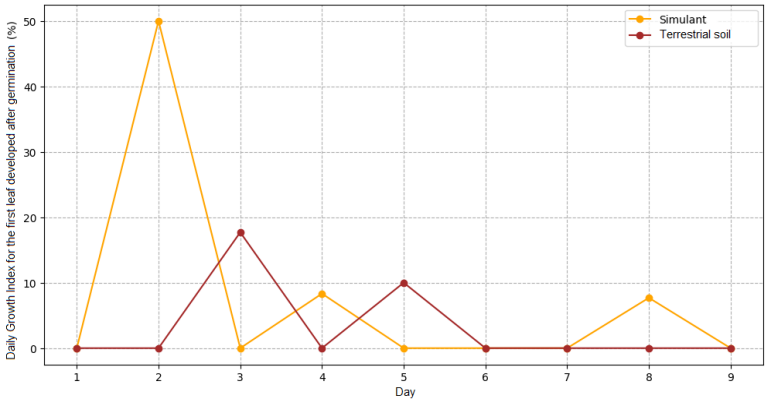

Fig 23: Daily Growth Index DGI_S over time for the first leaf developed after germination.

The graph shows the daily variation in percentage growth of leaf area DGI_S for the first leaf developed after germination, in plants grown in the martian simulant (orange line) and in terrestrial soil (brown line). The x-axis indicates time in days and the y-axis indicates DGI_S (%).

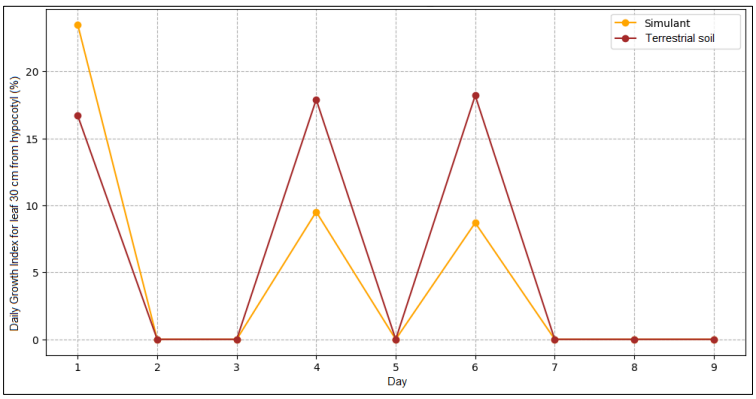

Fig 24: Daily Growth Index DGI_S over time for the leaf 30 cm from the hypocotyl.

The graph shows the daily variation in percentage growth of the leaf area DGI_S for the leaf developed 30 cm from the hypocotyl, in plants grown in the martian simulant (orange line) and in terrestrial soil (brown line). The x-axis indicates time (in days) and the y-axis the DGI_S (%).

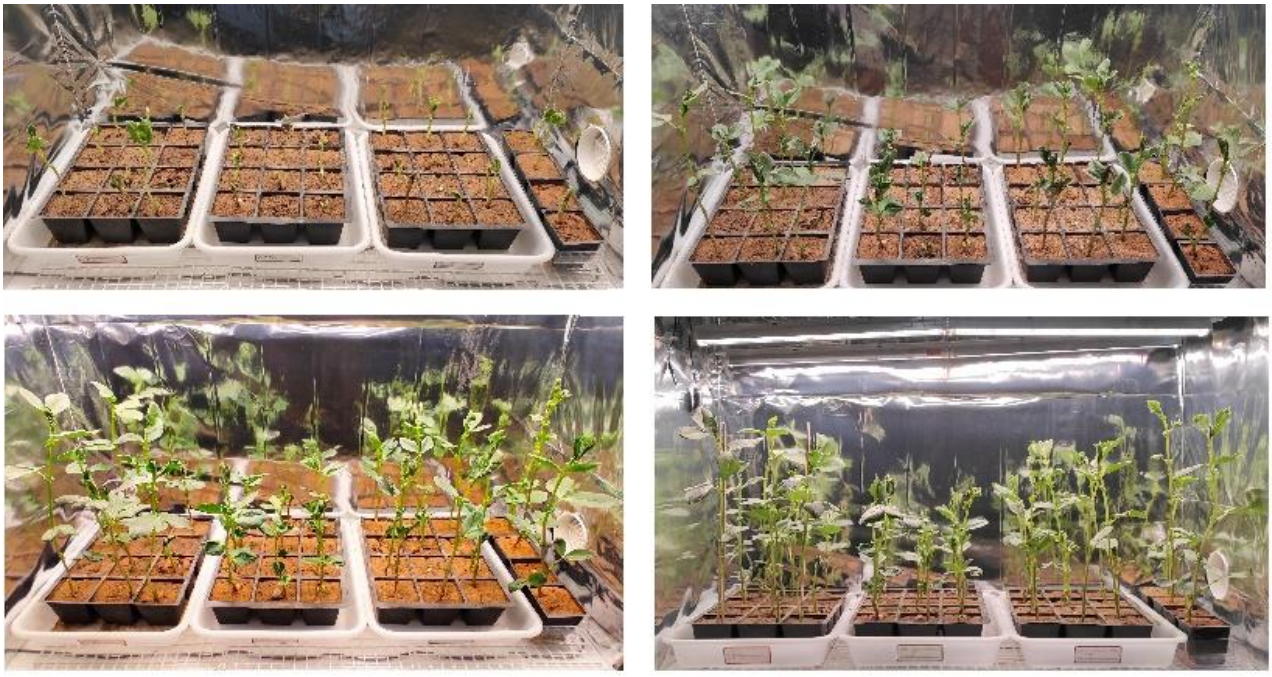

Fig 25: Some stages of plant development in the growth chamber.

Fresh weight, dry biomass and dry matter

In addition to height and leaf area measurements, we also assessed the dry biomass B_D of the plants, which represents the productivity and growth of the plant. The dry matter M_D was obtained by gently uprooting the plant, washing and drying the roots, and then drying it in an oven at 70 °C until it reached a constant weight. The M_D is measured in grams (g). A higher M_D indicates a larger and more developed plant. The dry matter M_D, which is the ratio between the dry biomass B_D and the fresh weight W_F of the plant, expressed as a percentage, was calculated:

$$M_D = \frac{B_D}{W_F} \times 100 \quad (7)$$

On average, we observed that for plants that reached a height of about 50 cm, the M_D was about 5% in the simulant and about 8% in the terrestrial soil. These data indicate a higher amount of M_D in plants grown in the terrestrial soil.

5. Discussion

Effects of pure simulant on the plant

When comparing the growth parameters of the sample plants in the simulant and in the terrestrial soil, a clear difference in overall development emerges, primarily due to the nutritional imbalances in the simulant.

The germination percentage (75%) of broad beans in the MSP-1 simulant aligns with the range (30-70%) observed for other nitrogen-fixing legumes in the simulant JSCMars-1A [6], while for nonleguminous plants (like lettuce and alfalfa), germination was ≥ 90% in both JSC-Mars-1A [7] and MMS-1 [7, 83]. In the MGS-1 simulant, germination was instead completely absent [7]. Both in the simulant and in the terrestrial soil, the plant broad bean relies on seed reserves for 8-12 days after germination before becoming dependent on the substrate.

In the simulant, plants initially displayed rapid growth rates (as shown in Figures 12 and 17, and Table 3), possibly due to the semi-controlled environment. However, they exhibited limited overall height and low biomass, likely due to the reduced total leaf area, which leads to decreased light-harvesting efficiency and photosynthesis. This seems to be caused by the deficiency of key nutrients, such as nitrogen, as observed in *Vigna aconitifolia*, a drought-resistant legume, in five different pure simulants [5]. These considerations are also supported by the analysis of the average daily increase of height, $ADGR_h$, which results in a slightly lower growth rate (1.67 cm/day) for the simulant compared to the terrestrial soil (1.87 cm/day).

Conversely, in terrestrial soil, which is rich in nutrients and organic matter, the initial growth rate may be slightly lower, but the plants develop fully and luxuriantly, as shown in Figure 26. This underscores the importance of environmental conditions and nutrients for plant growth. Plants in terrestrial soil exhibited healthy and robust growth, reaching abundant flowering, in contrast to the poor growth of the plants in the MSP-1 simulant, where flowering was nearly absent, as reported by other studies for legumes grown with JSC-Mars-1A [6].

The simulant plant also exhibited less leaf area growth than the one in terrestrial soil, as indicated by the trend lines in Figure 17 (relative to the first leaf) and Figure 20 (relative to the leaf at 30 cm), possibly related to nutrient availability, to limitations in photosynthesis due to low oxygen concentration, or to suboptimal artificial lighting in the growth chamber. The trend of the Daily Growth Index DGI_S in Figures 23 and 24 highlight how plant growth is discontinuous, and how the values vary depending on the position of the leaf (first or 30 cm from the hypocotyl) and on the time elapsed since germination, in particular in the first days after sprouting, as well as light and humidity conditions. The results of the analysis of the leaf area and the DGI_S reveal that the growth in terrestrial soil is faster and more effective during the initial growth, as shown by the steeper initial slope of the growth trend in Figure 17 and the higher peak of DGI_S in Figure 23.

Lettuce grown in pure MMS-1 simulant has shown a 5% lower development and a 9% reduced leaf area compared to plants fertilized at a 70:30 simulant:fertilizer ratio, while the dry matter was 17% higher, likely due to metal uptake from the pure simulant [84]. The lower leaves of the sample plants in the simulant exhibited yellowing and necrosis of the leaf margin after 40 to 50 days, as shown in Figure 27, which are symptoms of reduced calcium uptake due to salt and metal stress, as previously observed in sweetpotato plants subjected to high concentrations of MGS-1 simulant [3].

The average total biomass (expressed as dry matter) of the simulant plants was half that of the earth soil, in contrast to some nitrogen-fixing plants in which the biomass was greater in the JSC Mars-1A simulant than in the control soil, probably due to the higher water retention capacity and the presence of organic carbon, which promotes plant growth [6]. Similarly, for lettuce grown in pure MMS-1, the content of leaf dry matter was significantly higher (94%) than in mixtures treated with organic fertilizer. Stem sizes were also different, being about 4 mm for plants in the simulant, and 8 mm in plants in the terrestrial soil. The data relative to the surface fogliare, (summarized in Table 4) indicate that even if the growth index GI_S is slightly greater in the simulante, the *ADGRs* (the daily increase of area in mm²) is significantly higher in the terrestrial soil (83.3 mm²/day against 44.4 mm²/day), as well as the mean difference of the leaf area measured at 30 cm from the hypocotyl, which is of 511 mm² (as highlighted in Figure 22), confirming the higher growth of the plants in the terrestrial soil.

The limited plant growth in the simulant can be attributed to a combination of factors. First, the high pH of the simulant (8.50) compared to soil (7.27) may have affected the solubility and availability of some essential nutrients for plant growth, such as iron and phosphorus (Figure 6). The lower electrical conductivity E_C in the simulant (0.9 mS/cm) compared to soil (2.51 mS/cm) may indicate a lower concentration of soluble salts, potentially limiting nutrient supply. The lower redox potential E_h in the simulant (-90 mV) compared to soil (32 mV) may have affected the availability of some elements and microbial processes in the soil.

Furthermore, the higher porosity in the simulant (28.5% versus 6.3% in the soil) could have influenced water retention, aeration and nutrient availability, which in turn contributed to reduced plant growth (in the face of lower water retention). The text highlights that the lower capacity to absorb nutrients due to the simulant chemistry limits its productivity.

Finally, Table 2 highlights a granulometric composition that highlights how the simulant is mainly composed of silt and fine sand (75-85%), with a smaller part of clay (15-25%), suggesting a high draining capacity and a lower capacity to retain nutrients. In this situation, fertilization (which was not

used in this study) could have compensated for the limited water retention capacity.

Comparing these results with the chemical and physical composition of martian regolith reported by Ming and Morris [61], it can be noted that the simulant MSP-1 presents several differences, in particular a higher pH, a lower concentration of perchlorates, a lower electrical conductivity and the absence of organic matter. These differences could explain the different growth performance observed in the simulant compared to expectations based on knowledge of real martian surface. In particular, the lack of organic matter in the simulant may have limited the availability of nutrients and microbial activity in the soil, negatively affecting plant growth.

In conclusion, the results of the analysis show that while the simulated martian regolith (MSP-1) allows the germination and the early growth of plants, it does not provide a substrate where the plant reaches optimal development. As indicated by the lower values of $ADGR_h$ (Average Daily Growth Rate, related to height), *ADGRs* (Average Daily Growth Rate, related to the leaf area), and from the average lower values of biomass and dry substance, plant development in the simulant was less effective, compared to plants that developed in the terrestrial soil. The results suggest that this is likely due to a combination of factors related to the nutritional imbalance of the substrate.

Fig 26: Fava bean plants in the flowering stage, in martian simulant in environment semi-controlled and in earth soil under natural environmental conditions.

Fig 27: Yellowing and necrosis of the leaf margin. Progressive and complete yellowing of the paired leaf is also observed.

6. Conclusions

The results of this analysis show that, although the simulated Martian regolith (MSP-1) allows germination and early stages of plant growth, it does not provide a substrate in which the plant reaches optimal development. As evidenced by the lower values of $ADGR_h$ (Average Daily Growth Rate, relative to height), $ADGR_S$ (Average Daily Growth Rate, relative to leaf area), biomass, dry matter and chemical-physical properties, such as water retention and *pH*, plant development in the simulant was less effective than in terrestrial soil. The results suggest that the main causes are linked to a combination of factors, primarily a nutritional imbalance of the substrate.

The research presented in this article highlights the significant challenges associated with growing plants on Mars, an environment very different from Earth. The experiment on broad beans showed that although it is possible to achieve germination and growth of plants in the martian simulant, growth is generally lower than in natural soil, due to reasons related to nutritional imbalance.

These results highlight the importance of developing strategies to improve the fertility of the simulant, in order to obtain more effective results in future experiments. These strategies include the addition of specific nutrients, the

inoculation of microorganisms that enhance nutrient availability, and the addition of organic matter.

It is important to note that this study has limitations, including the use of a single type of simulant, a limited duration of the experiment (30 days), a low number of measurements per sample, and the absence of fertilization. Despite this, the importance of this experiment lies in its potential educational value, demonstrating how cultivation on Mars can be a fascinating and thought-provoking field of inquiry for students.

Growing plants on Mars is not simply a matter of overcoming technical challenges, but requires a holistic approach that takes into account the ethical, social and psychological implications of life on another planet. This approach will be crucial not only for the survival, but also for the well-being of future martian colonists. This study, despite its limitations, represents a first step towards the creation of a cultivable environment outside our planet and an important contribution to understanding the issues related to cultivation on Mars, with important implications for both scientific research in the field of astrobiology and for teaching. Through the described experiment, students can understand fundamental scientific concepts, such as soil properties, plant nutrition, photosynthesis and data analysis, developing critical thinking, problem-solving and collaboration skills. This work can therefore inspire future research, aimed at evaluating the effectiveness of different fertilization strategies and simulating even more realistic martian conditions, and promote innovative teaching activities that bring students closer to science and the challenges of the future.

6. References

1. Perchonok MR, Cooper MR, Catauro PM. Mission to Mars: food production and processing for the final frontier. Annu Rev Food Sci Technol. 2012;3(3):311-30.
2. Zabel P, *et al*. Review and analysis of over 40 years of space plant growth systems. LSSR. 2016;10:1-16.
3. Chinnannan K, *et al*. Effects of Mars Global Simulant (MGS-1) on Growth and Physiology of Sweet Potato: A Space Model Plant. Plants. 2024;13(1).
4. Fackrell LE, Schroeder PA. Growing plants on Mars: potential and limitations of martian regolith for in-situ resource utilization. Ninth International Conference on Mars 2019, LPI Contrib. No. 2089;6045.
5. Fackrell LE. Plant growth experiments using martian simulants: potential and limitations of agriculture on Mars. Lunar and Planetary Science Conference and Abstracts. 2021;1:Abstract 1634.
6. Wamelink GWW, *et al*. Can plants grow on Mars and the Moon: a growth experiment on Mars and Moon soil simulants. PLOS ONE. 2014;9(8):1-9.
7. Eichler A, *et al*. Challenging the agricultural viability of martian regolith simulants. Icarus. 2012;354:114022.
8. Rainwater R, Mukherjee A. The legume-rhizobia symbiosis can be supported on Mars soil simulants. PLOS ONE. 2021;16(12):1-10.
9. Harris F, *et al*. Soil fertility interactions with Sinorhizobium-legume symbiosis in a simulated Martian regolith; effects on nitrogen content and plant health. PLOS ONE. 2021;16(9):1-13.
10. Karl D, *et al*. Review of space resources processing for Mars missions: Martian simulants, regolith bonding concepts and additive manufacturing. Open Ceramics. 2022;9:100216.
11. Cannon KM, *et al*. Mars global simulant MGS-1: A Rocknest-based open standard for basaltic martian regolith simulants. Icarus. 2018;317:470-8.
12. Schuerger AC, *et al*. Biotoxicity of Mars soils: 1. Dry deposition of analog soils on microbial colonies and survival under Martian conditions. P&SS. 2012;72:91-101.
13. Schuerger AC, *et al*. Biotoxicity of Mars soils: 2. Survival of Bacillus subtilis and Enterococcus faecalis in aqueous extracts derived from six Mars analog soils. Icarus. 2017;290:215-23.
14. Zeng X, *et al*. JMSS-1: a new Martian soil simulant. Earth Planet Sp. 2015;67:72.
15. Stevens AH, *et al*. Y-Mars: An Astrobiological Analogue of Martian Mudstone. Earth & Planet Sci Lett. 2018;5:163-74.
16. Ramkissoon NK, *et al*. New simulants for martian regolith: Controlling iron variability. P&SS. 2019;179:104722.
17. Böttger U, *et al*. Optimizing the detection of carotene in cyanobacteria in a Martian regolith analogue with a Raman spectrometer for the ExoMars mission. P&SS. 2012;60(1):356-62.
18. Fackrell LE, *et al*. Development of martian regolith and bedrock simulants: Potential and limitations of martian regolith as an in-situ resource. Icarus. 2021;354:114055.
19. Rahim A, *et al*. WNMS: A New Basaltic Simulant of Mars Regolith. Sustainability. 2023;15(18).
20. Molar-Candanosa R. Growing green on the red planet. ACS ChemMatters. 2017;Apr/May:5-7.
21. Rapin W. Alternating wet and dry depositional environments recorded in the stratigraphy of Mount Sharp at Gale crater, Mars. Geology. 2021;49:842-6.
22. Audouard JF, *et al*. Water in the Martian regolith from OMEGA/Mars Express. J Geophys Res Planets. 2014;119:1969-89.
23. Jakosky BM, *et al*. Mars' atmospheric history derived from upper-atmosphere measurements of 38Ar/36Ar. Science. 2017;355(6332):1408-10.
24. Jakosky BM, *et al*. Loss of the Martian atmosphere to space: Present-day loss rates determined from MAVEN observations and integrated loss through time. Icarus. 2018;315:146-57.
25. Yokoo S, *et al*. Stratification in planetary cores by liquid immiscibility in Fe-S-H. Nat Commun. 2022;13(644).
26. Fedorova AA, *et al*. Stormy water on Mars: The distribution and saturation of atmospheric water during the dusty season. Science. 2020;367(6475):297-300.
27. Tian Z, *et al*. Potassium isotope composition of Mars reveals a mechanism of planetary volatile retention. PNAS. 2021;118(39):297-300.
28. Barlow NG. Mars. An introduction to its interior, surface and atmosphere. Cambridge: Cambridge University Press; 2008. p. 8, 164.
29. Catling DC. Chapter 16 - Mars Atmosphere: History and Surface Interactions in Encyclopedia of the Solar System. 3rd ed. Elsevier; 2014. p. 343–57.
30. Medina FJ, *et al*. Understanding Reduced Gravity Effects on Early Plant Development Before Attempting Life-Support Farming in the Moon and Mars. Front Astron Space Sci. 2021;8.
31. Hassler DM, *et al*. Mars' Surface Radiation Environment Measured with the Mars Science Laboratory's Curiosity Rover. Science. 2013;343(6169):798-804.

32. Pavlov A, *et al*. Sterilization of Martian surface by cosmic radiation. PSS. 2002;50:669-73.
33. Matthiä D, *et al*. The Martian surface radiation environment – a comparison of models and MSL/RAD measurements. JSWSC. 2016;6(A13).
34. Pavlov A, *et al*. Degradation of the organic molecules in the shallow subsurface of Mars due to irradiation by cosmic rays. Geophys Res Lett. 2012;39:669-73.
35. Dartnell LR, *et al*. Modelling the surface and subsurface Martian radiation environment: Implications for astrobiology. Geophys Res Lett. 2007;34:669-73.
36. Tack N, *et al*. Influence of Martian Radiation-like Conditions on the Growth of Secale cereale and Lepidium sativum. Front Astron Space Sci. 2021;8.
37. Hecht MH, *et al*. Detection of perchlorate and the soluble chemistry of martian soil at the Phoenix lander site. Science. 2009;325(5936):64-7.
38. Oze C, *et al*. Perchlorate and Agriculture on Mars. Soil Syst. 2021;5(37).
39. Brautigan D, *et al*. Aluminium speciation and phytotoxicity in alkaline soils. Plant Soil. 2012;360(11):329-34.
40. Stoker CR, *et al*. Habitability of the Phoenix landing site. J Geophys Res Planets. 2010;115(E6).
41. Smith PH, *et al*. H2O at the Phoenix Landing Site. Science. 2009;325(5936):58–61.
42. Dundas CM, *et al*. Exposed subsurface ice sheets in the Martian midlatitudes. Science. 2018;359(6372):199–201.
43. Poulet F, *et al*. Mineralogy of the Phoenix landing site from OMEGA observations and how that relates to in situ Phoenix measurements. Icarus. 2010;205:712–715.
44. Ehlmann BL, *et al*. Chemistry, mineralogy, and grain properties at Namib and High dunes, Bagnold dune field, Gale crater, Mars: A synthesis of Curiosity rover observations. J Geophys Res Planets. 2017;122:2510–2543.
45. Rennó NO. Possible physical and thermodynamical evidence for liquid water at the Phoenix landing site. J Geophys Res Planets. 2009;114(E1):E01–E07.
46. Lauro SE, *et al*. Using MARSIS signal attenuation to assess the presence of South Polar Layered Deposit subglacial brines. Nat Commun. 2022;13(5686):1–10.
47. Carter J, *et al*. A Mars orbital catalog of aqueous alteration signatures (MOCAAS). Icarus. 2023;389:1–16.
48. Riu L, Carter J, Poulet F. The M3 project: 3 – Global abundance distribution of hydrated silicates at Mars. Icarus. 2022;374:1–18.
49. Ojha L, *et al*. Spectral evidence for hydrated salts in recurring slope lineae on Mars. Nat Geosci. 2015;8:829–832.
50. McEwen AS, *et al*. Seasonal flows on warm Martian slopes. Science. 2009;333(6043):740–743.
51. Watters TR, *et al*. Evidence of ice-rich layered deposits in the Medusae Fossae Formation of Mars. Geophys Res Lett. 2024;51(1):740–743.
52. Zacny K, *et al*. RedWater: Approach for mining water from Mars' ice deposits buried tens of meters deep. Ninth International Conference on Mars. 2019;2089(6333):1–16.
53. DePasquale BM, Jenkins DM. The upper-thermal stability of an iron-rich smectite: Implications for smectite formation on Mars. Icarus. 2022;374:1–10.
54. Martín-Torres FJ, *et al*. Transient liquid water and water activity at Gale crater on Mars. Nat Geosci. 2015;8:357–361.
55. Hoffman S, Andrews A, Watts K. "Mining" Water Ice on Mars. An assessment of ISRU options in support of future human missions. Presentation of NTRS - NASA Technical Reports Server. 2016 Jul 1.
56. Schlehahn D, *et al*. Can a greenhouse be established on Mars? USURJ. 2017;4(09):1–12.
57. Bucklin RA, *et al*. Greenhouse design for the Mars environment. Acta Horticulturae. 2004;659(11):127–134.
58. Hublitz I, *et al*. Engineering concepts for inflatable Mars surface greenhouses. Adv Space Res. 2004;34(7):1546–1551.
59. Sauro F, *et al*. Lava tubes on Earth, Moon and Mars: A review on their size and morphology revealed by comparative planetology. Earth Sci Rev. 2020;209:1–17.
60. Sheshpari M, *et al*. Underground structures in Mars excavated by tunneling methods for sheltering humans. Tunn Undergr Space Technol. 2017;64:61–73.
61. Ming DW, Morris RV. Chemical, mineralogical, and physical properties of martian dust and soil. LPI Contributions. 2017;1966:6027.
62. Bariya H, *et al*. Boron: A promising nutrient for increasing growth and yield of plants. In: Nutrient Use Efficiency in Plants: Concepts and Approaches. New York: Springer International Publishing; 2014. p. 153–170.
63. McCollom TM, *et al*. Experimental serpentinization of iron-rich olivine (hortonolite): Implications for hydrogen generation and secondary mineralization on Mars and icy moons. Geochim Cosmochim Acta. 2022;335:98–110.
64. Burt DM. Iron-rich clay minerals on Mars: Potential sources or sinks for hydrogen and indicators of hydrogen loss over time. In: 19th Lunar and Planetary Science Conference. 1989. p. 423–432.
65. Navarro-González R, *et al*. Abiotic input of fixed nitrogen by bolide impacts to Gale crater during the Hesperian: Insights from the Mars Science Laboratory. J Geophys Res Planets. 2019;124:94–113.
66. Boxe CS, *et al*. An active nitrogen cycle on Mars sufficient to support a subsurface biosphere. Icarus. 2012;11(2):109–115.
67. Stern JC, *et al*. Evidence for indigenous nitrogen in sedimentary and aeolian deposits from the Curiosity rover investigations at Gale crater, Mars. Proc Natl Acad Sci U S A. 2015;112(14):4245–4250.
68. Davila AF, *et al*. Perchlorate on Mars: A chemical hazard and a resource for humans. Int J Astrobiol. 2013;12:321–325.
69. Zhu Q, *et al*. Automated synthesis of oxygen-producing catalysts from Martian meteorites by a robotic AI chemist. Nature Synthesis. 2023;1–7.
70. MacDonald JG, *et al*. An oxygen delivery polymer enhances seed germination in a Martian-like environment. Astrobiology. 2020;20:846–863.
71. Brückner J, *et al*. Mobility of phosphorus on the Martian surface and in a Martian meteorite. Astrobiology. 2009;40:1613.
72. Adcock CT, *et al*. Readily available phosphate from minerals in early aqueous environments on Mars. Nat Geosci. 2013;6:824–827.

73. Kounaves SP, *et al*. Soluble sulfate in the Martian soil at the Phoenix landing site. Geophys Res Lett. 2010;37(9):1–10.
74. Wentworth CK. A scale of grade and class terms for clastic sediments. J Geol. 1922;30(5):377–392.
75. Fukushi K, *et al*. Semiarid climate and hyposaline lake on early Mars inferred from reconstructed water chemistry at Gale. Nat Commun. 2019;10(10):1–9.
76. Quinn RC, *et al*. The oxidation-reduction potential of aqueous soil solutions at the Mars Phoenix landing site. Geophys Res Lett. 2011;38(7):1–10.
77. Mattila TJ. Redox potential as a soil health indicator – how does it compare to microbial activity and soil structure? Plant Soil. 2024;494:617–625.
78. Husson O. Redox potential (Eh) and pH as drivers of soil/plant/microorganism systems: A transdisciplinary overview pointing to integrative opportunities for agronomy. Plant Soil. 2012;362:389–417.
79. Kelova ME, *et al*. Human excreta as a resource in agriculture – Evaluating the fertilizer potential of different composting and fermentation-derived products. Resour Conserv Recycl. 2021;175:105748.
80. Zolotukhin IG, *et al*. Biological and physicochemical methods for utilization of plant wastes and human exometabolites for increasing internal cycling and closure of life support systems. Adv Space Res. 2005;35(9):1559–1562.
81. Wamelink G, *et al*. Growth of Rucola on Mars soil simulant under the influence of pig slurry and earthworms. Open Agric. 2022;7(1):238–248.
82. Lu Y, *et al*. Effects of drought and salt stress on seed germination of ephemeral plants in desert of northwest China. Front Ecol Evol. 2022;10:1–12.
83. Duri L, *et al*. Regolith as baseline to a future space farm. In: Proceedings of the 1st International Electronic Conference on Agronomy. 2021. p. 3–17.
84. Caporale AG, *et al*. Can lunar and Martian soils support food plant production? Effects of horse/swine monogastric manure fertilization on regolith simulants enzymatic activity, nutrient bioavailability, and lettuce growth. Plants. 2022;11(23):1–15.